PERGAMON

International Journal of Solids and Structures 40 (2003) 4585–4614

INTERNATIONAL JOURNAL OF SOLIDS and STRUCTURES

www.elsevier.com/locate/ijsolstr

A new 3-D finite element for nonlinear elasticity using the theory of a Cosserat point

B. Nadler, M.B. Rubin *

Faculty of Mechanical Engineering, Technion—Israel Institute of Technology, 32000 Haifa, Israel

Received 18 May 2002

Abstract

The theory of a Cosserat point has been used to formulate a new 3-D finite element for the numerical analysis of dynamic problems in nonlinear elasticity. The kinematics of this element are consistent with the standard tri-linear approximation in an eight node brick-element. Specifically, the Cosserat point is characterized by eight director vectors which are determined by balance laws and constitutive equations. For hyperelastic response, the constitutive equations for the director couples are determined by derivatives of a strain energy function. Restrictions are imposed on the strain energy function which ensure that the element satisfies a nonlinear version of the patch test. It is shown that the Cosserat balance laws are in one-to-one correspondence with those obtained using a Bubnov–Galerkin formulation. Nevertheless, there is an essential difference between the two approaches in the procedure for obtaining the strain energy function. Specifically, the Cosserat approach determines the constitutive coefficients for inhomogeneous deformations by comparison with exact solutions or experimental data. In contrast, the Bubnov–Galerkin approach determines these constitutive coefficients by integrating the 3-D strain energy function using the kinematic approximation. It is shown that the resulting Cosserat equations eliminate unphysical locking, and hourglassing in large compression without the need for using assumed enhanced strains or special weighting functions.

Keywords: Cosserat point; Numerical solution; 3-D element; Hourglassing; Nonlinear elasticity

1. Introduction

The finite element method has a long history. Huebner (1975) suggests that mathematicians, physicists and engineers each have legitimate claims to origins of the method in their own disciplines. In particular, he traces the origins back as far as Euler in 1774.

Another approach to the analysis of the dynamics of continuous media is based on a system of Cosserat-type bodies and can be traced back to the work of Wozniak (1973a), which is connected to his work on discrete elasticity (Wozniak, 1971, 1973b). Homogeneously deformable bodies have been analyzed as: zero-dimensional bodies (Slawianowski, 1974, 1975, 1982; Muncaster, 1984); as pseudo-rigid bodies (Cohen,

* Corresponding author. Fax: +972-4-829-5711.
E-mail address: mbrubin@tx.technion.ac.il (M.B. Rubin).

0020-7683/03/$ - see front matter © 2003 Elsevier Ltd. All rights reserved.
doi:10.1016/S0020-7683(03)00210-5

1981; Cohen and Muncaster, 1984a,b) and as Cosserat points (Rubin, 1985a). In particular, the work (Rubin, 1995, 1985a,b,) proposed the theory of a Cosserat point as a continuum theory for modeling finite elements in the numerical solution of problems in continuum mechanics. This numerical procedure based on the theory of a Cosserat point has been used to study the dynamics of strings (Rubin, 1987a; Rubin and Gottlieb, 1996) and spherically symmetric problems (Rubin, 1987b). More recently (Rubin, 2000, 2001), the theory of a Cosserat point has been generalized to model a fully nonlinear finite element for the numerical solution of dynamic 3-D motions of elastic beams. Also, Solberg and Papadopoulos (1999) have developed a finite element-based framework for the analysis of a collection of elastic pseudo-rigid bodies.

Papadopoulos (2001) has developed a higher-order model of a pseudo-rigid body which allows for a linear variation of the deformation gradient. This theory models the pseudo-rigid body with 30 degrees of freedom (six for rigid body motion, 24 for elastic deformations). In that work, the general structure for hyperelastic constitutive equations was considered in terms of volume integrals of a 3-D elastic strain energy function.

The rod element developed in (Rubin, 2000, 2001) cannot be used as a 3-D element because the cross-section of the rod is only allowed to experience general homogeneous deformation. Consequently, the objective of this paper is to develop an eight-node 3-D brick element based on the theory of a Cosserat point. Specifically, the theory is generalized to include eight director vectors with 24 degrees of freedom (six for rigid body motions and 18 for elastic deformations). It will be shown that a one-to-one correspondence exits between the balance laws of the Cosserat theory and weak forms of the equations developed using the Bubnov–Galerkin approximation procedure.

An essential difference between the Cosserat and the Bubnov–Galerkin approaches is the procedure that each uses to develop constitutive equations. For both approaches it is possible to develop hyperelastic constitutive equations for which the kinetic quantities are determined by derivatives of a strain energy function. In the Cosserat theory this strain energy is specified directly as a function of the independent variables and the constitutive coefficients are determined by comparison with exact solutions or experiments. In contrast, in the Bubnov–Galerkin approach this strain energy is determined by integrating the 3-D strain energy function with the assumption that the kinematic approximation is valid pointwise. It will be shown that even for the simple linear theory the constitutive coefficients obtained by each of these approaches are different. In particular, the Cosserat approach eliminates known unphysical locking phenomena that are caused by the Bubnov–Galerkin coefficients when no assumed enhanced strains or special weighting functions are used.

An outline of the paper is as follows. Section 2 describes the Cosserat direct approach, Section 3 introduces the kinematics of a general brick element and Section 4 discusses the Bubnov–Galerkin approach. Section 5 considers a nonlinear patch test, Section 6 develops the linearized equations, and Section 7 determines the constitutive coefficients for inhomogeneous deformations by considering the solution to problems of pure bending, pure torsion, and higher order hourglassing. Section 8 develops the nodal forms of the balance laws, Section 9 proposes the numerical solution procedure and Section 10 shows that hourglassing is absent in large compression. Section 11 summarizes the main results, and further details are provided in Appendices A–C.

Throughout the text, bold faced symbols are used to denote vector and tensor quantities. The symbol $\mathbf{I}$ denotes the unity tensor; $\mathrm{tr}(\mathbf{A})$ denotes the trace of the second order tensor $\mathbf{A}$; $\mathbf{A}^{\mathrm{T}}$ denotes the transpose of $\mathbf{A}$; $\mathbf{A}^{-1}$ denotes the inverse of $\mathbf{A}$; $\mathbf{A}^{-\mathrm{T}}$ denotes the inverse of the transpose of $\mathbf{A}$; and $\det(\mathbf{A})$ denotes the determinant of $\mathbf{A}$. The scalar $\mathbf{a}\cdot\mathbf{b}$ denotes the dot product between two vectors $\mathbf{a}$,$\mathbf{b}$; the scalar $\mathbf{A}\cdot\mathbf{B} = \mathrm{tr}(\mathbf{A}\mathbf{B}^{\mathrm{T}})$ denotes the dot product between two second order tensors $\mathbf{A}$,$\mathbf{B}$; the vector $\mathbf{a}\times\mathbf{b}$ denotes the cross product between $\mathbf{a}$ and $\mathbf{b}$; and the second-order tensor $\mathbf{a}\otimes\mathbf{b}$ denotes the tensor product between $\mathbf{a}$ and $\mathbf{b}$. Furthermore, since the range of indices varies depending on the context, the usual summation convention over repeated indices is suspended.

2. Direct approach for the balance laws of a Cosserat point

Within the context of the direct approach, the kinematics of the Cosserat point in its reference configuration are specified by eight constant director vectors $\mathbf{D}_i$ $(i = 0, 1, \ldots, 7)$. The vector $\mathbf{D}_0$ locates the Cosserat point relative to a fixed origin and the vectors $\mathbf{D}_i$ $(i = 1, 2, 3)$ are linearly independent

$$D^{1/2} = \mathbf{D}_1 \times \mathbf{D}_2 \cdot \mathbf{D}_3 > 0. \tag{2.1}$$

In its present configuration at time t, the Cosserat point is characterize by the eight director vectors $\mathbf{d}_i(t)$ and their velocities $\mathbf{w}_i$, which are both functions of time only

$$\mathbf{d}_i = \mathbf{d}_i(t), \quad \mathbf{w}_i = \dot{\mathbf{d}}_i \quad (i = 0, 1, \ldots, 7), \quad d^{1/2} = \mathbf{d}_1 \times \mathbf{d}_2 \cdot \mathbf{d}_3 > 0, \tag{2.2}$$

where a superposed dot denotes time differentiation. The kinetic quantities include the mass m and the constant director inertia coefficients y^{ij} (assumed to be a positive definite symmetric matrix)

$$y^{00} = 1, \quad y^{ij} = y^{ji}, \quad \dot{y}^{ij} = 0 \quad (i, j = 0, 1, \ldots, 7), \tag{2.3}$$

the assigned director couples $\mathbf{b}^i$ $(i = 0, 1, 2, \ldots, 7)$ due to body forces, the director couples $\mathbf{m}^i$ due to surface tractions on the boundaries of the Cosserat point, and the intrinsic director couples $\mathbf{t}^i$, which require constitutive equations.

Now, the conservation of mass and the balances of director momentum and angular momentum can be written in the forms, respectively,

$$\dot{m} = 0, \quad \frac{\mathrm{d}}{\mathrm{d}t}\left[\sum_{j=0}^{7} m y^{ij} \mathbf{w}_j\right] = m\mathbf{b}^i + \mathbf{m}^i - \mathbf{t}^i \quad \text{with} \quad \mathbf{t}^0 = 0, \tag{2.4a,b}$$

$$\frac{\mathrm{d}}{\mathrm{d}t}\left[\sum_{i=0}^{7}\sum_{j=0}^{7} \mathbf{d}_i \times m y^{ij} \mathbf{w}_j\right] = \sum_{i=0}^{7} \mathbf{d}_i \times m\mathbf{b}^i + \sum_{i=0}^{7} \mathbf{d}_i \times \mathbf{m}^i \quad (i = 0, 1, \ldots, 7). \tag{2.4c}$$

Moreover, with the help of (2.4b) it can be shown that the balance of angular momentum is satisfied provided that the tensor $\mathbf{T}$ is symmetric

$$\mathbf{T} = d^{-1/2} \sum_{i=1}^{7} \mathbf{t}^i \otimes \mathbf{d}_i = \mathbf{T}^{\mathrm{T}}. \tag{2.5}$$

Also, within the context of the purely mechanical theory, the kinetic energy $\mathscr{K}$, the rate of external work $\mathscr{W}$ done on the Cosserat point, and the rate of material dissipation $\mathscr{D}$ can be defined by

$$\mathscr{K} = \sum_{i=0}^{7}\sum_{j=0}^{7} \frac{1}{2} m y^{ij} \mathbf{w}_i \cdot \mathbf{w}_j, \quad \mathscr{W} = \sum_{i=0}^{7} m\mathbf{b}^i \cdot \mathbf{w}_i + \sum_{i=0}^{7} \mathbf{m}^i \cdot \mathbf{w}_i, \quad d^{1/2}\mathscr{D} = \mathscr{W} - \dot{\mathscr{K}} - m\dot{\Sigma} \geqslant 0, \tag{2.6}$$

where Σ is the specific strain energy function.

Next, by introducing the reciprocal vectors $\mathbf{D}^i$ and $\mathbf{d}^i$ $(i = 1, 2, 3)$ in terms of the Kronecker delta δ_i^j

$$\mathbf{D}_i \cdot \mathbf{D}^j = \delta_i^j, \quad \mathbf{d}_i \cdot \mathbf{d}^j = \delta_i^j \quad (i, j = 1, 2, 3), \tag{2.7}$$

it is possible to define the deformation tensor $\mathbf{F}$ and its determinant J

$$\mathbf{F} = \mathbf{F}(t) = \sum_{i=1}^{3} \mathbf{d}_i \otimes \mathbf{D}^i, \quad J = \det(\mathbf{F}) = \frac{d^{1/2}}{D^{1/2}} > 0, \tag{2.8}$$

as measures of homogeneous deformation, and define the vectors $\boldsymbol{\beta}_i$ $(i = 1, 2, 3, 4)$

$$\boldsymbol{\beta}_1 = \mathbf{F}^{-1}\mathbf{d}_4 - \mathbf{D}_4, \quad \boldsymbol{\beta}_2 = \mathbf{F}^{-1}\mathbf{d}_5 - \mathbf{D}_5, \quad \boldsymbol{\beta}_3 = \mathbf{F}^{-1}\mathbf{d}_6 - \mathbf{D}_6, \quad \boldsymbol{\beta}_4 = \mathbf{F}^{-1}\mathbf{d}_7 - \mathbf{D}_7, \tag{2.9}$$

as measures of inhomogeneous deformation. Furthermore, the rate of deformation tensor $\mathbf{L}$ and its symmetric part $\mathbf{D}$ are defined by

$$\mathbf{L} = \dot{\mathbf{F}}\mathbf{F}^{-1} = \sum_{i=1}^{3} \mathbf{w}_i \otimes \mathbf{d}^i, \quad \mathbf{D} = \frac{1}{2}(\mathbf{L} + \mathbf{L}^{\mathrm{T}}) = \mathbf{D}^{\mathrm{T}}. \tag{2.10}$$

Then, the equations of motion (2.4) can be used to reduce the rate of dissipation to the form

$$d^{1/2}\mathscr{D} = d^{1/2}\mathbf{T} \cdot \mathbf{D} + \sum_{i=1}^{4} \mathbf{F}^{\mathrm{T}}\mathbf{t}^{(i+3)} \cdot \dot{\boldsymbol{\beta}}_i - m\dot{\Sigma} \geqslant 0. \tag{2.11}$$

For a nonlinear anisotropic elastic Cosserat point, the strain energy function can be written in the form

$$\Sigma = \Sigma(\mathbf{C}, \boldsymbol{\beta}_i), \quad \mathbf{C} = \mathbf{F}^{\mathrm{T}}\mathbf{F}, \tag{2.12}$$

$\mathbf{T}$ and $\mathbf{t}^i$ are independent of the rate $\mathbf{L}$, and the rate of dissipation vanishes so that $\mathbf{T}$ and $\mathbf{t}^i$ are determined by the hyperelastic constitutive equations

$$d^{1/2}\mathbf{T} = 2m\mathbf{F}\frac{\partial \Sigma}{\partial \mathbf{C}}\mathbf{F}^{\mathrm{T}}, \quad \mathbf{t}^{(i+3)} = m\mathbf{F}^{-\mathrm{T}}\frac{\partial \Sigma}{\partial \boldsymbol{\beta}_i} \quad (i = 1, 2, 3, 4), \tag{2.13a,b}$$

$$\mathbf{t}^i = \left[d^{1/2}\mathbf{T} - \sum_{j=4}^{7} \mathbf{t}^j \otimes \mathbf{d}_j\right] \cdot \mathbf{d}^i \quad (i = 1, 2, 3). \tag{2.13c}$$

Moreover, it can be shown that the kinematic and kinetic quantities in the Cosserat theory are properly invariant under superposed rigid body motions. In particular, $\mathbf{d}_i$ $(i = 1, 2, \ldots, 7)$ and $\mathbf{F}$ are rotated and $\mathbf{C}$ and $\boldsymbol{\beta}_i$ are unaltered by superposed rigid body motions.

3. A general brick element

For a general brick element with eight nodes a material point in the stress-free reference configuration is located by the vector $\mathbf{X}^*$ using the tri-linear representation

$$\mathbf{X}^*(\theta^1, \theta^2, \theta^3) = \sum_{j=0}^{7} N^j(\theta^1, \theta^2, \theta^3)\mathbf{D}_j, \tag{3.1}$$

where θ^i $(i = 1, 2, 3)$ are convected coordinates and N^i are shape functions

$$\begin{aligned} &N^0 = 1, \quad N^1 = \theta^1, \quad N^2 = \theta^2, \quad N^3 = \theta^3, \\ &N^4 = \theta^1\theta^2, \quad N^5 = \theta^1\theta^3, \quad N^6 = \theta^2\theta^3, \quad N^7 = \theta^1\theta^2\theta^3. \end{aligned} \tag{3.2}$$

Similarly, the same material point in the present configuration is located by the vector $\mathbf{x}^*$ expressed in the form

$$\mathbf{x}^*(\theta^1, \theta^2, \theta^3, t) = \sum_{j=0}^{7} N^j(\theta^1, \theta^2, \theta^3)\mathbf{d}_j(t). \tag{3.3}$$

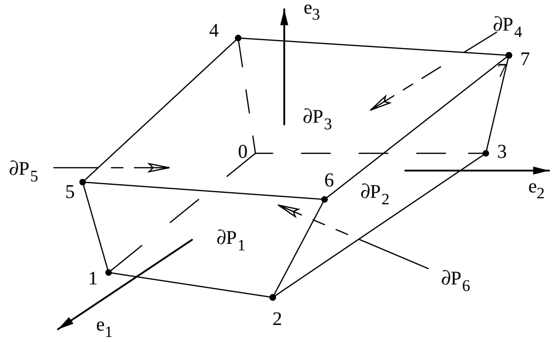

Fig. 1. Sketch of a general eight-node brick element showing the numbering of the nodes and the surfaces.

Moreover, the brick region P is bounded by the six surfaces ∂P_J ($J = 1, 2, \ldots, 6$), such that (Fig. 1)

$$|\theta^1| \leqslant \frac{H}{2}, \quad |\theta^2| \leqslant \frac{W}{2}, \quad |\theta^3| \leqslant \frac{L}{2},$$
$$\theta^1 = \frac{H}{2} \text{ on } \partial P_1, \quad \theta^2 = \frac{W}{2} \text{ on } \partial P_2, \quad \theta^3 = \frac{L}{2} \text{ on } \partial P_3, \tag{3.4}$$
$$\theta^1 = -\frac{H}{2} \text{ on } \partial P_4, \quad \theta^2 = -\frac{W}{2} \text{ on } \partial P_5, \quad \theta^3 = -\frac{L}{2} \text{ on } \partial P_6,$$

where $\{H, L, W\}$ are constant lengths. Thus, the directors $\mathbf{D}_i$ and $\mathbf{d}_i(t)$ are related to the vectors $\overline{\mathbf{D}}_i$ and $\overline{\mathbf{d}}_i(t)$ ($i = 0, 1, \ldots, 7$) which locate the nodes in the reference and present configurations, respectively, by the constant matrix A_{ij} given in Appendix A, such that

$$\mathbf{D}_i = \sum_{j=0}^{7} A_{ij}\overline{\mathbf{D}}_j, \qquad \mathbf{d}_i = \sum_{j=0}^{7} A_{ij}\overline{\mathbf{d}}_j. \tag{3.5}$$

Moreover, it is noted that the values of the nodal vectors $\overline{\mathbf{D}}_i$ and $\overline{\mathbf{d}}_i$ are limited by the assumption that the representations (3.1) and (3.3) remain invertible. Furthermore, in view of these tri-linear representations, the surfaces ∂P_J need not be planar and can have a bi-linear dependence on the surface coordinates.

4. Bubnov–Galerkin approach

Using the definitions given in Green and Adkins (1960), the conservation of mass and the balance of linear momentum can be written as

$$m^* = m^*(\theta^i) = \rho^* g^{1/2}, \quad m^*\dot{\mathbf{v}}^* = m^*\mathbf{b}^* + \mathbf{t}^{*j}_{,j}, \tag{4.1a,b}$$

where m^* is independent of time, ρ^* is the current mass density, $\mathbf{v}^* = \dot{\mathbf{x}}^*$ is the absolute velocity, $\mathbf{b}^*$ is the specific (per unit mass) body force, a superposed dot denotes material time differentiation holding θ^i fixed, the vectors $\mathbf{t}^{*j}$ are related to the Cauchy stress tensor $\mathbf{T}^*$ by the formula

$$\mathbf{t}^{*j} = g^{1/2}\mathbf{T}^*\mathbf{g}^j \tag{4.2}$$

and the reference covariant base vectors $\mathbf{G}_i$, their reciprocal vectors $\mathbf{G}^i$, the present covariant base vectors $\mathbf{g}_i$, and their reciprocal vectors $\mathbf{g}^i$ are specified by

$$\mathbf{G}_i = \mathbf{X}^*_{,i}, \quad \mathbf{G}_i \cdot \mathbf{G}^i = \delta^j_i, \quad G^{1/2} = \mathbf{G}_1 \times \mathbf{G}_2 \cdot \mathbf{G}_3 > 0,$$

$$\mathbf{g}_i = \mathbf{x}^*_{,i}, \quad \mathbf{g}_i \cdot \mathbf{g}^i = \delta^j_i, \quad g^{1/2} = \mathbf{g}_1 \times \mathbf{g}_2 \cdot \mathbf{g}_3 > 0 \qquad (i,j = 1,2,3), \tag{4.3}$$

where a comma denotes partial differentiation with respect to θ^i. Also, a superscript (*) is used to distinguish quantities related to the 3-D theory from those related to the Cosserat theory.

Now, following the standard Bubnov–Galerkin approximation, (4.1b) is multiplied by the shape function N^i, the representation (3.3) is used and the result is integrated over the region P of the element to obtain weak forms of the balance of linear momentum. In particular, using the definitions

$$my^{ij} = \int_P \rho^* N^i N^j \mathrm{d}v^*, \quad m\mathbf{b}^i = \int_P [N^i \rho^* \mathbf{b}^*]\, \mathrm{d}v^*, \quad \mathbf{m}^i_J = \int_{\partial P_J} N^i \mathbf{t}^* \mathrm{d}a^*, \tag{4.4a–c}$$

$$\mathbf{m}^i = \sum_{J=1}^{6} \mathbf{m}^i_J, \quad \mathbf{t}^i = \sum_{m=1}^{3} \int_P [N^i_{,m} g^{-1/2} \mathbf{t}^{*m}]\, \mathrm{d}v^* \quad (i,j = 0,1,\ldots,7) \;\; (J = 1,2,\ldots,6). \tag{4.4d,e}$$

It can be shown that the resulting weak equations are in one-to-one correspondence with the balance laws (2.4b) of the Cosserat theory. In these equations $\mathrm{d}v^*$ is the volume element and $\mathrm{d}a^*$ is the area element in the present configuration. Also, with the help of the representation (3.3) and the definitions (4.4) it can be shown that the global form of the balance of angular momentum is identical to the Cosserat balance law (2.4c).

For a hyperelastic 3-D material the Cauchy stress $\mathbf{T}^*$ is related to the strain energy Σ^* and the 3-D deformation gradient $\mathbf{F}^*$ by the formulas

$$\Sigma^* = \Sigma^*(\mathbf{C}^*), \quad \mathbf{F}^* = \sum_{i=1}^{3} \mathbf{g}_i \otimes \mathbf{G}^i, \quad \mathbf{C}^* = \mathbf{F}^{*\mathrm{T}}\mathbf{F}^*, \quad \mathbf{T}^* = 2\rho^* \mathbf{F}^* \frac{\partial \Sigma^*}{\partial \mathbf{C}^*} \mathbf{F}^{*\mathrm{T}}. \tag{4.5}$$

It then follows that within the context of the Bubnov–Galerkin approach the constitutive equations for $\mathbf{t}^i$ can be written in the forms (2.13) where the strain energy function Σ is specified by

$$m\Sigma = \int_P \rho^* \Sigma^*(\mathbf{C}^*)\, \mathrm{d}v^*. \tag{4.6}$$

It is emphasized that in evaluating the integral in (4.6) the kinematic representations (3.1) and (3.3) are assumed to valid pointwise in the region P. Moreover, for general element shapes and general nonlinear strain energy functions it is necessary to evaluate this integral numerically. In contrast, within the context of the Cosserat theory the dependence of strain energy function Σ on the variables $\{\mathbf{C}, \boldsymbol{\beta}_i\}$ is proposed directly and the constitutive constants and functions are determined by comparison with exact solutions of the 3-D theory or experimental data. It will be shown later that even for the simple case of the linear theory of a rectangular parallelepiped element the constitutive coefficients obtained in these two approaches are significantly different.

For later reference it is noted that in view of the definitions (4.4c) and the specifications (3.4) only 24 of the 48 vectors $\mathbf{m}^i_J$ are independent since

$$
\begin{aligned}
&\mathbf{m}_1^1 = \frac{H}{2}\mathbf{m}_1^0, \quad \mathbf{m}_1^4 = \frac{H}{2}\mathbf{m}_1^2, \quad \mathbf{m}_1^5 = \frac{H}{2}\mathbf{m}_1^3, \quad \mathbf{m}_1^7 = \frac{H}{2}\mathbf{m}_1^6,\\
&\mathbf{m}_2^2 = \frac{W}{2}\mathbf{m}_2^0, \quad \mathbf{m}_2^4 = \frac{W}{2}\mathbf{m}_2^1, \quad \mathbf{m}_2^6 = \frac{W}{2}\mathbf{m}_2^3, \quad \mathbf{m}_2^7 = \frac{W}{2}\mathbf{m}_2^5,\\
&\mathbf{m}_3^3 = \frac{L}{2}\mathbf{m}_3^0, \quad \mathbf{m}_3^5 = \frac{L}{2}\mathbf{m}_3^1, \quad \mathbf{m}_3^6 = \frac{L}{2}\mathbf{m}_3^2, \quad \mathbf{m}_3^7 = \frac{L}{2}\mathbf{m}_3^4,\\
&\mathbf{m}_4^1 = -\frac{H}{2}\mathbf{m}_4^0, \quad \mathbf{m}_4^4 = -\frac{H}{2}\mathbf{m}_4^2, \quad \mathbf{m}_4^5 = -\frac{H}{2}\mathbf{m}_4^3, \quad \mathbf{m}_4^7 = -\frac{H}{2}\mathbf{m}_4^6,\\
&\mathbf{m}_5^2 = -\frac{W}{2}\mathbf{m}_5^0, \quad \mathbf{m}_5^4 = -\frac{W}{2}\mathbf{m}_5^1, \quad \mathbf{m}_5^6 = -\frac{W}{2}\mathbf{m}_5^3, \quad \mathbf{m}_5^7 = -\frac{W}{2}\mathbf{m}_5^5,\\
&\mathbf{m}_6^3 = -\frac{L}{2}\mathbf{m}_6^0, \quad \mathbf{m}_6^5 = -\frac{L}{2}\mathbf{m}_6^1, \quad \mathbf{m}_6^6 = -\frac{L}{2}\mathbf{m}_6^2, \quad \mathbf{m}_6^7 = -\frac{L}{2}\mathbf{m}_6^4.
\end{aligned} \tag{4.7}
$$

Also, it is convenient to define the position vectors $\hat{\mathbf{d}}_J$ to the centroids of the surfaces ∂P_J, and define the moments $\hat{\mathbf{m}}_J$ applied to the surfaces ∂P_J (about the points $\hat{\mathbf{d}}_J$) by the expressions

$$
\hat{\mathbf{m}}_J = \sum_{i=0}^{7} \mathbf{d}_i \times \mathbf{m}_J^i - \hat{\mathbf{d}}_J \times \mathbf{m}_J^0 \quad (J = 1, 2, \ldots, 6), \tag{4.8}
$$

where it is noted that $\mathbf{m}_J^0$ represents the total force applied to ∂P_J.

5. A nonlinear patch test

Following previous research on shells (Naghdi and Rubin, 1995), rods (Rubin, 1996) and points (Rubin, 2000, 2001) it is possible to impose restrictions on the strain energy function Σ which ensure that the theory of a Cosserat point produces solutions that are consistent with the exact 3-D theory for all homogeneous deformations of an arbitrary uniform homogeneous anisotropic elastic material. These restrictions are equivalent to a nonlinear patch test on the brick element. Specifically, confining attention to such a material it can be shown that the mass m is given by

$$
m = \rho_0^* D^{1/2} V \tag{5.1}
$$

and the restrictions on Σ require

$$
\frac{\partial \Sigma(\mathbf{C}, \boldsymbol{\beta}_i)}{\partial \mathbf{C}} = \frac{\partial \Sigma^*(\mathbf{C})}{\partial \mathbf{C}}, \qquad \frac{\partial \Sigma(\mathbf{C}, \boldsymbol{\beta}_j)}{\partial \boldsymbol{\beta}_i} = 2\mathbf{C}\frac{\partial \Sigma^*(\mathbf{C})}{\partial \mathbf{C}}\mathbf{V}^i \quad \text{for } \boldsymbol{\beta}_i = 0 \;\; (i = 1, 2, 3, 4), \tag{5.2}
$$

where V and $\mathbf{V}^i$ are constants defined by Eq. (B.2). In particular, it can be shown that the 3-D deformation is homogeneous if and only if $\boldsymbol{\beta}_i$ vanish, which leads to $\mathbf{F}^* = \mathbf{F}$. Consequently, $\boldsymbol{\beta}_i$ are measures of inhomogeneous deformations.

The restrictions (5.2) can be simplified by introducing the auxiliary variables

$$
\overline{\mathbf{F}} = \overline{\mathbf{F}}(\mathbf{F}, \boldsymbol{\beta}_i; \mathbf{V}^i) = \mathbf{F}\left[\mathbf{I} + \sum_{m=1}^{4} \boldsymbol{\beta}_m \otimes \mathbf{V}^m\right], \quad \overline{\mathbf{C}} = \overline{\mathbf{F}}^{\mathrm{T}}\overline{\mathbf{F}} \tag{5.3}
$$

and writing the strain energy function in the form

$$
\Sigma(\mathbf{C}, \boldsymbol{\beta}_i) = \Sigma^*(\overline{\mathbf{C}}) + \Psi(\mathbf{C}, \boldsymbol{\beta}_i) \quad (i = 1, 2, 3, 4). \tag{5.4}
$$

Using this representation, the restrictions (5.2) require the strain energy of inhomogeneous deformations Ψ to satisfy the equations

$$\frac{\partial \Psi(\mathbf{C},\boldsymbol{\beta}_i)}{\partial \mathbf{C}} = 0, \qquad \frac{\partial \Psi(\mathbf{C},\boldsymbol{\beta}_i)}{\partial \boldsymbol{\beta}_m} = 0 \qquad \text{for} \quad \boldsymbol{\beta}_i = 0 \ \ (i,m = 1,2,3,4). \tag{5.5}$$

The representation (5.4) is valid for a general elastic material with strain energy Σ^*. Unfortunately, general restrictions are not known which determine Ψ in terms of Σ^* and the geometry of the structure. Therefore, in order to develop a specific form for Ψ it is necessary to consider specific materials. To this end, attention is focused on a 3-D isotropic material and use is made of the work of Flory (1961), which defines a pure measure of distortional deformation. Within this context, a simple model for a generalized compressible Neo-Hookean material can be characterized by the strain energy function

$$2\rho_0^*\Sigma^*(\overline{\mathbf{C}}) = 2K^*[\overline{J} - 1 - \ln(\overline{J})] + \mu^*(\overline{\mathbf{C}}' \cdot \mathbf{I} - 3), \tag{5.6}$$

where K^* is the bulk modulus, μ^* is the shear modulus, and the pure measures of distortional deformation are defined by the unimodular tensors $\{\overline{\mathbf{F}}', \overline{\mathbf{C}}', \overline{\mathbf{B}}'\}$, such that

$$\overline{\mathbf{F}}' = \overline{J}^{-1/3}\overline{\mathbf{F}}, \quad \overline{J} = \det(\overline{\mathbf{F}}), \quad \overline{\mathbf{C}}' = \overline{\mathbf{F}}'^{\mathrm{T}}\overline{\mathbf{F}}', \quad \overline{\mathbf{B}}' = \overline{\mathbf{F}}'\overline{\mathbf{F}}'^{\mathrm{T}}. \tag{5.7}$$

Moreover, it can be shown that

$$2m\frac{\partial \Sigma^*(\overline{\mathbf{C}})}{\partial \overline{\mathbf{C}}} = D^{1/2}V\left[K^*(\overline{J} - 1)\overline{\mathbf{C}}^{-1} + \mu^*\overline{J}^{-2/3}\left\{\mathbf{I} - \frac{1}{3}(\overline{\mathbf{C}} \cdot \mathbf{I})\overline{\mathbf{C}}^{-1}\right\}\right]. \tag{5.8}$$

Next, it is convenient to introduce the normalized inhomogeneous strain measures

$$\begin{aligned}
&\kappa_1^1 = W\boldsymbol{\beta}_1 \cdot \mathbf{D}^1, \quad \kappa_1^2 = H\boldsymbol{\beta}_1 \cdot \mathbf{D}^2, \quad \kappa_1^3 = L\boldsymbol{\beta}_1 \cdot \mathbf{D}^3,\\
&\kappa_2^1 = L\boldsymbol{\beta}_2 \cdot \mathbf{D}^1, \quad \kappa_2^2 = W\boldsymbol{\beta}_2 \cdot \mathbf{D}^2, \quad \kappa_2^3 = H\boldsymbol{\beta}_2 \cdot \mathbf{D}^3,\\
&\kappa_3^1 = H\boldsymbol{\beta}_3 \cdot \mathbf{D}^1, \quad \kappa_3^2 = L\boldsymbol{\beta}_3 \cdot \mathbf{D}^2, \quad \kappa_3^3 = W\boldsymbol{\beta}_3 \cdot \mathbf{D}^3,\\
&\kappa_4^1 = WL\boldsymbol{\beta}_4 \cdot \mathbf{D}^1, \quad \kappa_4^2 = HL\boldsymbol{\beta}_4 \cdot \mathbf{D}^2, \quad \kappa_4^3 = HW\boldsymbol{\beta}_4 \cdot \mathbf{D}^3.
\end{aligned} \tag{5.9}$$

Then, as a special case, the inhomogeneous strain energy Ψ is assumed to be independent of $\overline{\mathbf{C}}$ and is taken as a quadratic function of the strains κ_j^i $(i = 1,2,3;\ j = 1,2,3,4)$ of the form

$$\begin{aligned}
2m\Psi = D^{1/2}V[&K_1(\kappa_1^1)^2 + 2K_2(\kappa_1^1\kappa_3^3) + K_3(\kappa_3^3)^2 + K_4(\kappa_1^2)^2 + 2K_5(\kappa_1^2\kappa_2^3) + K_6(\kappa_2^3)^2 + K_7(\kappa_2^1)^2\\
&+ 2K_8(\kappa_2^1\kappa_3^2) + K_9(\kappa_3^2)^2 + K_{10}(\kappa_1^3)^2 + K_{11}(\kappa_2^2)^2 + K_{12}(\kappa_3^1)^2 + 2K_{13}(\kappa_1^3\kappa_2^2) + 2K_{14}(\kappa_1^3\kappa_3^1)\\
&+ 2K_{15}(\kappa_2^2\kappa_3^1) + K_{16}(\kappa_4^1)^2 + K_{17}(\kappa_4^2)^2 + K_{18}(\kappa_4^3)^2],
\end{aligned} \tag{5.10}$$

where $\{K_1–K_{18}\}$ are constants to be determined in terms of material and geometric quantities. Furthermore, using the strain energy representations (5.4), (5.6) and (5.10) the constitutive equations (2.13) yield

$$
\begin{aligned}
d^{1/2}\mathbf{T} &= D^{1/2}V\left[K^*(\bar{J}-1)\mathbf{I} + \mu^*\left\{\overline{\mathbf{B}}' - \frac{1}{3}(\overline{\mathbf{B}}'\cdot\mathbf{I})\mathbf{I}\right\}\right],\\
\mathbf{t}^4 &= D^{1/2}V\left[K^*(\bar{J}-1)\overline{\mathbf{F}}^{-\mathrm{T}} + \mu^*\bar{J}^{-2/3}\left\{\overline{\mathbf{F}} - \frac{1}{3}(\overline{\mathbf{B}}\cdot\mathbf{I})\overline{\mathbf{F}}^{-\mathrm{T}}\right\}\right]\mathbf{V}^1\\
&\quad + D^{1/2}V\left[W\{K_1\kappa_1^1 + K_2\kappa_3^3\}\mathbf{d}^1 + H\{K_4\kappa_1^2 + K_5\kappa_2^3\}\mathbf{d}^2 + L\{K_{10}\kappa_1^3 + K_{13}\kappa_2^2 + K_{14}\kappa_3^1\}\mathbf{d}^3\right],\\
\mathbf{t}^5 &= D^{1/2}V\left[K^*(\bar{J}-1)\overline{\mathbf{F}}^{-\mathrm{T}} + \mu^*\bar{J}^{-2/3}\left\{\overline{\mathbf{F}} - \frac{1}{3}(\overline{\mathbf{B}}\cdot\mathbf{I})\overline{\mathbf{F}}^{-\mathrm{T}}\right\}\right]\mathbf{V}^2\\
&\quad + D^{1/2}V\left[L\{K_7\kappa_2^1 + K_8\kappa_3^2\}\mathbf{d}^1 + W\{K_{11}\kappa_2^2 + K_{13}\kappa_1^3 + K_{15}\kappa_3^1\}\mathbf{d}^2 + H\{K_5\kappa_1^2 + K_6\kappa_2^3\}\mathbf{d}^3\right],\\
\mathbf{t}^6 &= D^{1/2}V\left[K^*(\bar{J}-1)\overline{\mathbf{F}}^{-\mathrm{T}} + \mu^*\bar{J}^{-2/3}\left\{\overline{\mathbf{F}} - \frac{1}{3}(\overline{\mathbf{B}}\cdot\mathbf{I})\overline{\mathbf{F}}^{-\mathrm{T}}\right\}\right]\mathbf{V}^3\\
&\quad + D^{1/2}V\left[H\{K_{12}\kappa_3^1 + K_{14}\kappa_1^3 + K_{15}\kappa_2^2\}\mathbf{d}^1 + L\{K_8\kappa_2^1 + K_9\kappa_3^2\}\mathbf{d}^2 + W\{K_2\kappa_1^1 + K_3\kappa_3^3\}\mathbf{d}^3\right],\\
\mathbf{t}^7 &= D^{1/2}V\left[K^*(\bar{J}-1)\overline{\mathbf{F}}^{-\mathrm{T}} + \mu^*\bar{J}^{-2/3}\left\{\overline{\mathbf{F}} - \frac{1}{3}(\overline{\mathbf{B}}\cdot\mathbf{I})\overline{\mathbf{F}}^{-\mathrm{T}}\right\}\right]\mathbf{V}^4\\
&\quad + D^{1/2}V\left[WL\{K_{16}\kappa_4^1\}\mathbf{d}^1 + HL\{K_{17}\kappa_4^2\}\mathbf{d}^2 + HW\{K_{18}\kappa_4^3\}\mathbf{d}^3\right],
\end{aligned}
\tag{5.11}
$$

where the remainder of $\mathbf{t}^i$ are determined by (2.13c).

6. Linearized equations

The equations of motion (2.4) and the constitutive equations (2.13) are valid for large deformations and large rotations of the Cosserat point. The objective of this section is to develop simplified forms of these equations which are limited to small strains, displacements and rotations. To this end, the director displacements $\boldsymbol{\delta}_i$ are introduced, such that

$$\mathbf{d}_i = \mathbf{D}_i + \boldsymbol{\delta}_i \quad (i = 0, 1, \ldots, 7). \tag{6.1}$$

In addition, it is assumed that these displacements and the kinetic quantities

$$\{\mathbf{b}^i, \mathbf{m}^i, \mathbf{t}^i\} \quad (i = 0, 1, \ldots, 7) \tag{6.2}$$

remain small enough that quadratic terms in these quantities can be neglected relative to linear terms. It then follows that the equations of motion (2.4b) can be written as

$$\sum_{j=0}^{7} m y^{ij} \ddot{\boldsymbol{\delta}}_j = m\mathbf{b}^i + \mathbf{m}^i - \mathbf{t}^i \text{ with } (\mathbf{t}^0 = 0) \quad (i = 0, 1, \ldots, 7). \tag{6.3}$$

Next, using (6.1) and neglecting quadratic terms in $\boldsymbol{\delta}_i$ it can be shown that the kinematic quantities can be approximated by

$$
\begin{aligned}
&d^{1/2} = D^{1/2}\left[1 + \sum_{i=1}^{3}\boldsymbol{\delta}_i\cdot\mathbf{D}^i\right], \quad \mathbf{F} = \mathbf{I} + \sum_{i=1}^{3}\boldsymbol{\delta}_i\otimes\mathbf{D}^i, \quad J = 1 + \sum_{i=1}^{3}\boldsymbol{\delta}_i\cdot\mathbf{D}^i,\\
&\overline{\mathbf{F}} = \left[\mathbf{I} + \sum_{i=1}^{3}\boldsymbol{\delta}_i\otimes\mathbf{D}^i + \sum_{m=1}^{4}\boldsymbol{\beta}_m\otimes\mathbf{V}^m\right], \quad \bar{J} = 1 + \sum_{i=1}^{3}\boldsymbol{\delta}_i\cdot\mathbf{D}^i + \sum_{m=1}^{4}\boldsymbol{\beta}_m\cdot\mathbf{V}^m,\\
&\boldsymbol{\beta}_1 = \boldsymbol{\delta}_4 - \sum_{i=1}^{3}(\mathbf{D}_4\cdot\mathbf{D}^i)\boldsymbol{\delta}_i, \quad \boldsymbol{\beta}_2 = \boldsymbol{\delta}_5 - \sum_{i=1}^{3}(\mathbf{D}_5\cdot\mathbf{D}^i)\boldsymbol{\delta}_i,\\
&\boldsymbol{\beta}_3 = \boldsymbol{\delta}_6 - \sum_{i=1}^{3}(\mathbf{D}_6\cdot\mathbf{D}^i)\boldsymbol{\delta}_i, \quad \boldsymbol{\beta}_4 = \boldsymbol{\delta}_7 - \sum_{i=1}^{3}(\mathbf{D}_7\cdot\mathbf{D}^i)\boldsymbol{\delta}_i,
\end{aligned}
\tag{6.4}
$$

so that the linearized forms of the constitutive equations (5.11) become

$$\begin{aligned}
\mathbf{T} &= VK^*\left[\sum_{i=1}^{3}\boldsymbol{\delta}_i\cdot\mathbf{D}^i+\sum_{m=1}^{4}\boldsymbol{\beta}_m\cdot\mathbf{V}^m\right]\mathbf{I}+V\mu^*\left[\sum_{i=1}^{3}\left\{\boldsymbol{\delta}_i\otimes\mathbf{D}^i+\mathbf{D}^i\otimes\boldsymbol{\delta}_i-\frac{2}{3}(\boldsymbol{\delta}_i\cdot\mathbf{D}^i)\mathbf{I}\right\}\right.\\
&\qquad\left.+\sum_{m=1}^{4}\left\{\boldsymbol{\beta}_m\otimes\mathbf{V}^m+\mathbf{V}^m\otimes\boldsymbol{\beta}_m-\frac{2}{3}(\boldsymbol{\beta}_m\cdot\mathbf{V}^m)\mathbf{I}\right\}\right],\\
\mathbf{t}^4 &= D^{1/2}\mathbf{T}\mathbf{V}^1+D^{1/2}V\big[W\{K_1\kappa_1^1+K_2\kappa_3^3\}\mathbf{D}^1+H\{K_4\kappa_1^2+K_5\kappa_2^3\}\mathbf{D}^2+L\{K_{10}\kappa_1^3+K_{13}\kappa_2^2+K_{14}\kappa_3^1\}\mathbf{D}^3\big],\\
\mathbf{t}^5 &= D^{1/2}\mathbf{T}\mathbf{V}^2+D^{1/2}V[L\{K_7\kappa_2^1+K_8\kappa_3^2\}\mathbf{D}^1+W\{K_{11}\kappa_2^2+K_{13}\kappa_1^3+K_{15}\kappa_3^1\}\mathbf{D}^2+H\{K_5\kappa_1^2+K_6\kappa_2^3\}\mathbf{D}^3],\\
\mathbf{t}^6 &= D^{1/2}\mathbf{T}\mathbf{V}^3+D^{1/2}V[H\{K_{12}\kappa_3^1+K_{14}\kappa_1^3+K_{15}\kappa_2^2\}\mathbf{D}^1+L\{K_8\kappa_2^1+K_9\kappa_3^2\}\mathbf{D}^2+W\{K_2\kappa_1^1+K_3\kappa_3^3\}\mathbf{D}^3],\\
\mathbf{t}^7 &= D^{1/2}\mathbf{T}\mathbf{V}^4+D^{1/2}V[WL\{K_{16}\kappa_4^1\}\mathbf{D}^1+HL\{K_{17}\kappa_4^2\}\mathbf{D}^2+HW\{K_{18}\kappa_4^3\}\mathbf{D}^3],\\
\mathbf{t}^i &= \left[D^{1/2}\mathbf{T}-\sum_{j=4}^{7}\mathbf{t}^j\otimes\mathbf{D}_j\right]\cdot\mathbf{D}^i\quad(i=1,2,3).
\end{aligned}\tag{6.5}$$

Furthermore, the linearized forms of the moments defined in (4.8) become

$$\hat{\mathbf{m}}_J=\sum_{i=0}^{7}\mathbf{D}_i\times\mathbf{m}_J^i-\widehat{\mathbf{D}}_J\times\mathbf{m}_J^0\quad(J=1,2,\ldots,6),\tag{6.6}$$

where $\widehat{\mathbf{D}}_J$ are the reference values of $\hat{\mathbf{d}}_J$.

7. Determination of the constitutive constants

The theory of a Cosserat point with the constitutive equations (5.4), (5.6), (5.10) and (5.11) requires specification of the reference directors

$$\mathbf{D}_i\quad(i=0,1,\ldots,7),\tag{7.1}$$

the inertia quantities

$$\{m,y^{ij}\}\quad(i,j=0,1,\ldots 7),\tag{7.2}$$

the isotropic 3-D material constants

$$\{K^*,\mu^*\}\tag{7.3}$$

and the constitutive constants

$$\{K_1\text{–}K_9\},\quad\{K_{10}\text{–}K_{15}\},\quad\{K_{16}\text{–}K_{18}\},\tag{7.4a–c}$$

associated with inhomogeneous deformations. Also, it is necessary to specify the assigned director couples $\mathbf{b}^i$.

These constitutive equations are valid for large deformations and large rotations but they also must produce reasonable results for small deformations. Consequently, values for the constitutive constants $\{K_1\text{–}K_{18}\}$ can be determined by comparing Cosserat solutions with exact solutions of the linearized 3-D theory of a rectangular parallelepiped. Once these constitutive constants have been determined they are used in the nonlinear constitutive equations to predict the response of the Cosserat point to general deformations and for general reference shapes of the brick element.

In the previous sections the Cosserat point has been considered to be a general brick element in its reference configuration. Here and throughout the remainder of the text, attention is focused on a Cosserat point which is a rectangular parallelepiped in its reference configuration. For this case the reference directors $\mathbf{D}_i$ can be specified such that

$$\mathbf{D}_1 = \mathbf{D}^1 = \mathbf{e}_1, \quad \mathbf{D}_2 = \mathbf{D}^2 = \mathbf{e}_2, \quad \mathbf{D}_3 = \mathbf{D}^3 = \mathbf{e}_3, \quad \mathbf{D}_4 = \mathbf{D}_5 = \mathbf{D}_6 = \mathbf{D}_7 = 0, \tag{7.5}$$

where $\mathbf{e}_i$ $(i = 1, 2, 3)$ are constant orthonormal base vectors. Using these specifications it follows from (2.1) and (B.2) that

$$D^{1/2} = 1, \quad V = HWL, \quad \mathbf{V}^i = 0 \ \ (i = 1, 2, 3, 4). \tag{7.6}$$

It will be shown presently that the constants (7.4a) can be determined by comparing Cosserat solutions with exact linear solutions for pure bending, the constants (7.4b) can be determined by considering solutions of pure torsion, and the constants (7.4c) can be determined by considering an exact higher-order hourglass-type solution.

The kinematic assumption (3.3) and the definition (6.1) suggest that the 3-D displacement field $\mathbf{u}^*(\theta^1, \theta^2, \theta^3, t)$ is approximated by

$$\mathbf{u}^* = \boldsymbol{\delta}_0 + \theta^1\boldsymbol{\delta}_1 + \theta^2\boldsymbol{\delta}_2 + \theta^3\boldsymbol{\delta}_3 + \theta^1\theta^2\boldsymbol{\delta}_4 + \theta^1\theta^3\boldsymbol{\delta}_5 + \theta^2\theta^3\boldsymbol{\delta}_6 + \theta^1\theta^2\theta^3\boldsymbol{\delta}_7. \tag{7.7}$$

However, usually this expression is not general enough to reproduce exact solutions. Therefore, even when the exact 3-D solution of a problem is known, it is necessary to propose some procedure for determining the associated kinematic and kinetic quantities in the Cosserat theory. This problem has been discussed within the context of beam equations (Rubin, 1996, 2002) and a procedure has been proposed to relate the director displacements to integrals of the exact 3-D displacement field $\mathbf{u}^*$. An important characteristic of this procedure is that it preserves the functional form of the integrated stress–strain relations. Here, this procedure is generalized and the director displacements $\boldsymbol{\delta}_i$ are compared with the exact expressions $\boldsymbol{\delta}_i^*(t)$ defined by

$$\begin{gathered}
V^* = \int_P \mathrm{d}V^* = \int_{-L/2}^{L/2}\int_{-W/2}^{W/2}\int_{-H/2}^{H/2} \mathrm{d}\theta^1\mathrm{d}\theta^2\mathrm{d}\theta^3 = V = HWL, \\
\boldsymbol{\delta}_0^*(t) = \frac{1}{V^*}\int_P \mathbf{u}^*\mathrm{d}V^*, \quad \boldsymbol{\delta}_i^*(t) = \frac{1}{V^*}\int_P \frac{\partial\mathbf{u}^*}{\partial\theta^i}\mathrm{d}V^* \ \ (i = 1, 2, 3), \\
\boldsymbol{\delta}_4^*(t) = \frac{1}{V^*}\int_P \frac{\partial^2\mathbf{u}^*}{\partial\theta^1\partial\theta^2}\mathrm{d}V^*, \quad \boldsymbol{\delta}_5^*(t) = \frac{1}{V^*}\int_P \frac{\partial^2\mathbf{u}^*}{\partial\theta^1\partial\theta^3}\mathrm{d}V^*, \\
\boldsymbol{\delta}_6^*(t) = \frac{1}{V^*}\int_P \frac{\partial^2\mathbf{u}^*}{\partial\theta^2\partial\theta^3}\mathrm{d}V^*, \quad \boldsymbol{\delta}_7^*(t) = \frac{1}{V^*}\int_P \frac{\partial^3\mathbf{u}^*}{\partial\theta^1\partial\theta^2\partial\theta^3}\mathrm{d}V^*.
\end{gathered} \tag{7.8}$$

Moreover, motivated by the definitions (4.4c), the Cosserat quantities $\mathbf{m}_J^i$ are compared with the exact integrated effects $\mathbf{m}_J^{i*}$ of the surface tractions which are given by

$$
\begin{aligned}
\mathbf{m}_1^{i^*} &= \sum_{j=1}^{3} \int_{-L/2}^{L/2} \int_{-W/2}^{W/2} N^i\left(\frac{H}{2}, \theta^2, \theta^3\right) T_{1j}^*\left(\frac{H}{2}, \theta^2, \theta^3, t\right) \mathbf{e}_j \, \mathrm{d}\theta^2 \, \mathrm{d}\theta^3 \quad (i = 0, 2, 3, 6), \\
\mathbf{m}_2^{i^*} &= \sum_{j=1}^{3} \int_{-L/2}^{L/2} \int_{-H/2}^{H/2} N^i\left(\theta^1, \frac{W}{2}, \theta^3\right) T_{2j}^*\left(\theta^1, \frac{W}{2}, \theta^3, t\right) \mathbf{e}_j \, \mathrm{d}\theta^1 \, \mathrm{d}\theta^3 \quad (i = 0, 1, 3, 5), \\
\mathbf{m}_3^{i^*} &= \sum_{j=1}^{3} \int_{-W/2}^{W/2} \int_{-H/2}^{H/2} N^i\left(\theta^1, \theta^2, \frac{L}{2}\right) T_{3j}^*\left(\theta^1, \theta^2, \frac{L}{2}, t\right) \mathbf{e}_j \, \mathrm{d}\theta^1 \, \mathrm{d}\theta^2 \quad (i = 0, 1, 2, 4), \\
\mathbf{m}_4^{i^*} &= -\sum_{j=1}^{3} \int_{-L/2}^{L/2} \int_{-W/2}^{W/2} N^i\left(-\frac{H}{2}, \theta^2, \theta^3\right) T_{1j}^*\left(-\frac{H}{2}, \theta^2, \theta^3, t\right) \mathbf{e}_j \, \mathrm{d}\theta^2 \, \mathrm{d}\theta^3 \quad (i = 0, 2, 3, 6), \\
\mathbf{m}_5^{i^*} &= -\sum_{j=1}^{3} \int_{-L/2}^{L/2} \int_{-H/2}^{H/2} N^i\left(\theta^1, -\frac{W}{2}, \theta^3\right) T_{2j}^*\left(\theta^1, -\frac{W}{2}, \theta^3, t\right) \mathbf{e}_j \, \mathrm{d}\theta^1 \, \mathrm{d}\theta^3 \quad (i = 0, 1, 3, 5) \\
\mathbf{m}_6^{i^*} &= -\sum_{j=1}^{3} \int_{-W/2}^{W/2} \int_{-H/2}^{H/2} N^i\left(\theta^1, \theta^2, -\frac{L}{2}\right) T_{3j}^*\left(\theta^1, \theta^2, -\frac{L}{2}, t\right) \mathbf{e}_j \, \mathrm{d}\theta^1 \, \mathrm{d}\theta^2 \quad (i = 0, 1, 2, 4),
\end{aligned}
\tag{7.9}
$$

in terms of the shape functions (3.2) and the components T_{ij}^* of the Cauchy stress $\mathbf{T}^*$ relative to the basis $\mathbf{e}_i$. These expressions are consistent with Eqs. (4.7). Also, it is convenient to use of the formulas (4.4d) and (6.6) to define the exact kinetic quantities

$$
\mathbf{m}^{i*} = \sum_{J=1}^{6} \mathbf{m}_J^{i^*}, \qquad \hat{\mathbf{m}}_J^* = \sum_{i=0}^{7} \mathbf{D}_i \times \mathbf{m}_J^{i^*} - \hat{\mathbf{D}}_J \times \mathbf{m}_J^{0^*} \quad (J = 1, 2, \ldots, 6). \tag{7.10}
$$

7.1. Pure bending

The solution of the equilibrium of a rectangular parallelepiped subjected to pure bending with no body force is well known (e.g. Sokolnikoff, 1956). For the general case, there are six independent solutions which correspond to bending moments applied in two orthogonal directions on each of the three sets of opposing surfaces, and a summary of Lekhnitskii's solution (1963) for orthotropic materials can be found in Section 3.14 of Rubin (2000). Using this solution (with L interchanged with H) and specializing it to the case of isotropic materials it can be shown with the help of (7.8)–(7.10) that the values $\boldsymbol{\delta}_i^*$, $\mathbf{m}^{i^*}$ and $\hat{\mathbf{m}}_J^*$ become

$$
\begin{aligned}
&\boldsymbol{\delta}_0^* = 0, \quad \boldsymbol{\delta}_1^* = 0, \quad \boldsymbol{\delta}_2^* = 0, \quad \boldsymbol{\delta}_3^* = 0, \quad \boldsymbol{\delta}_7^* = 0, \\
&\boldsymbol{\delta}_4^* = \left[\left\{\frac{12M_{21}}{E^*W^3L}\right\} - v^*\left\{\frac{12M_{23}}{E^*HW^3}\right\}\right]\mathbf{e}_1 + \left[\left\{\frac{12M_{12}}{E^*H^3L}\right\} - v^*\left\{\frac{12M_{13}}{E^*H^3W}\right\}\right]\mathbf{e}_2, \\
&\boldsymbol{\delta}_5^* = \left[\left\{\frac{12M_{31}}{E^*WL^3}\right\} - v^*\left\{\frac{12M_{32}}{E^*HL^3}\right\}\right]\mathbf{e}_1 + \left[-v^*\left\{\frac{12M_{12}}{E^*H^3L}\right\} + \left\{\frac{12M_{13}}{E^*H^3W}\right\}\right]\mathbf{e}_3, \\
&\boldsymbol{\delta}_6^* = \left[-v^*\left\{\frac{12M_{31}}{E^*WL^3}\right\} + \left\{\frac{12M_{32}}{E^*HL^3}\right\}\right]\mathbf{e}_2 + \left[-v^*\left\{\frac{12M_{21}}{E^*W^3L}\right\} + \left\{\frac{12M_{23}}{E^*HW^3}\right\}\right]\mathbf{e}_3, \\
&\mathbf{m}^{0^*} = \mathbf{m}^{1^*} = \mathbf{m}^{2^*} = \mathbf{m}^{3^*} = \mathbf{m}^{7^*} = 0, \\
&\mathbf{m}^{4*} = HM_{21}\mathbf{e}_1 + WM_{12}\mathbf{e}_2, \quad \mathbf{m}^{5*} = HM_{31}\mathbf{e}_1 + LM_{13}\mathbf{e}_3, \quad \mathbf{m}^{6*} = WM_{32}\mathbf{e}_2 + LM_{23}\mathbf{e}_3, \\
&\hat{\mathbf{m}}_1^* = M_{31}\mathbf{e}_2 - M_{21}\mathbf{e}_3, \quad \hat{\mathbf{m}}_2^* = -M_{32}\mathbf{e}_1 + M_{12}\mathbf{e}_3, \quad \hat{\mathbf{m}}_3^* = M_{23}\mathbf{e}_1 - M_{13}\mathbf{e}_2, \\
&\hat{\mathbf{m}}_4^* = M_{31}\mathbf{e}_2 + M_{21}\mathbf{e}_3, \quad \hat{\mathbf{m}}_5^* = M_{32}\mathbf{e}_1 - M_{12}\mathbf{e}_3, \quad \hat{\mathbf{m}}_3^* = -M_{23}\mathbf{e}_1 + M_{13}\mathbf{e}_2,
\end{aligned}
\tag{7.11}
$$

where the rigid body displacements and rotations have been chosen so that $\{\boldsymbol{\delta}_0^*, \boldsymbol{\delta}_1^*, \boldsymbol{\delta}_2^*, \boldsymbol{\delta}_3^*\}$ vanish, $\{M_{21}, M_{31}, M_{12}, M_{32}, M_{13}, M_{23}\}$ are constant moments, E^* is Young's modulus and v^* is Poisson's ratio, which are related to K^* and μ^* by the expressions

$$K^* = \frac{2\mu^*(1+v^*)}{3(1-2v^*)}, \quad E^* = 2\mu^*(1+v^*). \tag{7.12}$$

In view of these results, the problem of pure bending in the Cosserat theory is formulated by specifying

$$\begin{aligned} &\mathbf{m}^i = \mathbf{m}^{i*}, \quad \mathbf{b}^i = 0, \quad \boldsymbol{\delta}_0 = \boldsymbol{\delta}_1 = \boldsymbol{\delta}_2 = \boldsymbol{\delta}_3 = \boldsymbol{\delta}_7 = 0, \\ &\kappa_1^3 = \kappa_2^2 = \kappa_3^1 = \kappa_4^1 = \kappa_4^2 = \kappa_4^3 = 0, \quad \text{all other } \kappa_j^i \text{ are nonzero.} \end{aligned} \tag{7.13}$$

Then, using (5.9), (6.4), (6.5), (7.5) and (7.6) the nontrivial equilibrium equations (6.3) can be solved for the kinematic variables to obtain

$$\begin{aligned} &\kappa_1^1 = \frac{K_3\left\{\dfrac{M_{21}}{W^2L}\right\} - K_2\left\{\dfrac{M_{23}}{HW^2}\right\}}{K_1K_3 - K_2K_2}, \quad \kappa_3^3 = \frac{-K_2\left\{\dfrac{M_{21}}{W^2L}\right\} + K_1\left\{\dfrac{M_{23}}{HW^2}\right\}}{K_1K_3 - K_2K_2}, \\ &\kappa_1^2 = \frac{K_6\left\{\dfrac{M_{12}}{H^2L}\right\} - K_5\left\{\dfrac{M_{13}}{H^2W}\right\}}{K_4K_6 - K_5K_5}, \quad \kappa_2^3 = \frac{-K_5\left\{\dfrac{M_{12}}{H^2L}\right\} + K_4\left\{\dfrac{M_{13}}{H^2W}\right\}}{K_4K_6 - K_5K_5}, \\ &\kappa_2^1 = \frac{K_9\left\{\dfrac{M_{31}}{WL^2}\right\} - K_8\left\{\dfrac{M_{32}}{HL^2}\right\}}{K_7K_9 - K_8K_8}, \quad \kappa_3^2 = \frac{-K_8\left\{\dfrac{M_{31}}{WL^2}\right\} + K_7\left\{\dfrac{M_{32}}{HL^2}\right\}}{K_7K_9 - K_8K_8}. \end{aligned} \tag{7.14}$$

Moreover, it can easily be seen that this Cosserat solution will be consistent with the exact solution (7.11) provided that the constitutive constants $\{K_1–K_9\}$ are specified by the values given in Table 1. This table also includes the coefficients predicted by the Bubnov–Galerkin solution described in Appendix C.

7.2. Pure torsion

The solution of the equilibrium of a rectangular parallelepiped subjected to pure torsion with no body force is well known (e.g. Sokolnikoff, 1956). For the general case there are three independent solutions which correspond to torsional moments applied perpendicular to each of the three sets of opposing surfaces and a summary of Lekhnitskii's solution (1963) for orthotropic materials can be found in Rubin (2000, Section 3.15). Using this solution (with L interchanged with H) and specializing it to the case of isotropic materials it can be shown with the help of (7.8)–(7.10) that the values $\boldsymbol{\delta}_i^*$, $\mathbf{m}^{i*}$ and $\hat{\mathbf{m}}_J^*$ become

Table 1
Comparison of the Cosserat and Bubnov–Galerkin values of the constitutive coefficients

	Cosserat	Bubnov–Galerkin
K_1	$\frac{E^*}{12(1-\nu^{*2})}$	$\left[\frac{E^*}{12(1-\nu^{*2})}\right]\left[\frac{(1-\nu^*)^2}{1-2\nu^*}+\left\{\frac{1-\nu^*}{2}\right\}\frac{H^2}{W^2}\right]$
K_2	$\frac{\nu^*E^*}{12(1-\nu^{*2})}$	$\left[\frac{\nu^*E^*}{12(1-\nu^{*2})}\right]\left[\frac{1-\nu^*}{1-2\nu^*}\right]$
K_3	$\frac{E^*}{12(1-\nu^{*2})}$	$\left[\frac{E^*}{12(1-\nu^{*2})}\right]\left[\frac{(1-\nu^*)^2}{1-2\nu^*}+\left\{\frac{1-\nu^*}{2}\right\}\frac{L^2}{W^2}\right]$
K_4	$\frac{E^*}{12(1-\nu^{*2})}$	$\left[\frac{E^*}{12(1-\nu^{*2})}\right]\left[\frac{(1-\nu^*)^2}{1-2\nu^*}+\left\{\frac{1-\nu^*}{2}\right\}\frac{W^2}{H^2}\right]$
K_5	$\frac{\nu^*E^*}{12(1-\nu^{*2})}$	$\left[\frac{\nu^*E^*}{12(1-\nu^{*2})}\right]\left[\frac{1-\nu^*}{1-2\nu^*}\right]$
K_6	$\frac{E^*}{12(1-\nu^{*2})}$	$\left[\frac{E^*}{12(1-\nu^{*2})}\right]\left[\frac{(1-\nu^*)^2}{1-2\nu^*}+\left\{\frac{1-\nu^*}{2}\right\}\frac{L^2}{H^2}\right]$
K_7	$\frac{E^*}{12(1-\nu^{*2})}$	$\left[\frac{E^*}{12(1-\nu^{*2})}\right]\left[\frac{(1-\nu^*)^2}{1-2\nu^*}+\left\{\frac{1-\nu^*}{2}\right\}\frac{H^2}{L^2}\right]$
K_8	$\frac{\nu^*E^*}{12(1-\nu^{*2})}$	$\left[\frac{\nu^*E^*}{12(1-\nu^{*2})}\right]\left[\frac{1-\nu^*}{1-2\nu^*}\right]$
K_9	$\frac{E^*}{12(1-\nu^{*2})}$	$\left[\frac{E^*}{12(1-\nu^{*2})}\right]\left[\frac{(1-\nu^*)^2}{1-2\nu^*}+\left\{\frac{1-\nu^*}{2}\right\}\frac{W^2}{L^2}\right]$
K_{10}	$\frac{\mu^*}{6}\left[\frac{H^2+W^2}{L^2}\right]b^*(1)$	$\frac{\mu^*}{12}\left[\frac{H^2+W^2}{L^2}\right]$
K_{11}	$\frac{\mu^*}{6}\left[\frac{H^2+L^2}{W^2}\right]b^*(1)$	$\frac{\mu^*}{12}\left[\frac{H^2+L^2}{W^2}\right]$
K_{12}	$\frac{\mu^*}{6}\left[\frac{W^2+L^2}{H^2}\right]b^*(1)$	$\frac{\mu^*}{12}\left[\frac{W^2+L^2}{H^2}\right]$
K_{13}	$\frac{\mu^*}{6}\left[\frac{H^2}{WL}\right]b^*(1)$	$\frac{\mu^*}{12}\left[\frac{H^2}{WL}\right]$
K_{14}	$\frac{\mu^*}{6}\left[\frac{W^2}{HL}\right]b^*(1)$	$\frac{\mu^*}{12}\left[\frac{W^2}{HL}\right]$
K_{15}	$\frac{\mu^*}{6}\left[\frac{L^2}{HW}\right]b^*(1)$	$\frac{\mu^*}{12}\left[\frac{L^2}{HW}\right]$
K_{16}	$\frac{\mu^*}{144}\left[\frac{2(3-\nu^*)}{(3-2\nu^*)}+\frac{H^2}{W^2}+\frac{H^2}{L^2}\right]$	$\frac{\mu^*}{144}\left[\frac{2(1-\nu^*)}{(1-2\nu^*)}+\frac{H^2}{W^2}+\frac{H^2}{L^2}\right]$
K_{17}	$\frac{\mu^*}{144}\left[\frac{2(3-\nu^*)}{(3-2\nu^*)}+\frac{W^2}{H^2}+\frac{W^2}{L^2}\right]$	$\frac{\mu^*}{144}\left[\frac{2(1-\nu^*)}{(1-2\nu^*)}+\frac{W^2}{H^2}+\frac{W^2}{L^2}\right]$
K_{18}	$\frac{\mu^*}{144}\left[\frac{2(3-\nu^*)}{(3-2\nu^*)}+\frac{L^2}{H^2}+\frac{L^2}{W^2}\right]$	$\frac{\mu^*}{144}\left[\frac{2(1-\nu^*)}{(1-2\nu^*)}+\frac{L^2}{H^2}+\frac{L^2}{W^2}\right]$

$$
\begin{aligned}
&\boldsymbol{\delta}_0^* = \boldsymbol{\delta}_1^* = \boldsymbol{\delta}_2^* = \boldsymbol{\delta}_3^* = \boldsymbol{\delta}_7^* = 0,\\
&\boldsymbol{\delta}_4^* = [\omega_1^* - \omega_2^* - \omega_3^*\Phi_3^*]\mathbf{e}_3, \quad \boldsymbol{\delta}_5^* = [-\omega_1^* + \omega_2^*\Phi_2^* + \omega_3^*]\mathbf{e}_2, \quad \boldsymbol{\delta}_6^* = [-\omega_1^*\Phi_1^* + \omega_2^* - \omega_3^*]\mathbf{e}_1,\\
&\Phi^*(\xi) = 1 - \sum_{n=1}^{\infty}\left[\frac{32}{\pi^3(2n-1)^3\xi}\right]\tanh\left[\frac{\pi(2n-1)\xi}{2}\right] = -\Phi^*\left(\frac{1}{\xi}\right),\\
&\Phi_1^* = \Phi^*\left(\frac{W}{L}\right) \quad \text{for } \frac{W}{L} \leqslant 1, \quad \Phi_1^* = -\Phi^*\left(\frac{L}{W}\right) \quad \text{for } \frac{W}{L} > 1,\\
&\Phi_2^* = \Phi^*\left(\frac{H}{L}\right) \quad \text{for } \frac{H}{L} \leqslant 1, \quad \Phi_2^* = -\Phi^*\left(\frac{L}{H}\right) \quad \text{for } \frac{H}{L} > 1,\\
&\Phi_3^* = \Phi^*\left(\frac{H}{W}\right) \quad \text{for } \frac{H}{W} \leqslant 1, \quad \Phi_3^* = -\Phi^*\left(\frac{W}{H}\right) \quad \text{for } \frac{H}{W} > 1,\\
&\mathbf{m}^{0*} = \mathbf{m}^{1*} = \mathbf{m}^{2*} = \mathbf{m}^{3*} = \mathbf{m}^{7*} = 0, \quad \mathbf{m}^{4*} = \frac{1}{2}(HT_1 - WT_2)\mathbf{e}_3,\\
&\mathbf{m}^{5*} = \frac{1}{2}(-HT_1 + LT_3)\mathbf{e}_2, \quad \mathbf{m}^{6*} = \frac{1}{2}(WT_2 - LT_3)\mathbf{e}_1,\\
&\hat{\mathbf{m}}_1^* = -\hat{\mathbf{m}}_4^* = T_1\mathbf{e}_1, \quad \hat{\mathbf{m}}_2^* = -\hat{\mathbf{m}}_5^* = T_2\mathbf{e}_2, \quad \hat{\mathbf{m}}_3^* = -\hat{\mathbf{m}}_6^* = T_3\mathbf{e}_3,
\end{aligned}
\tag{7.15}
$$

where Φ_i^* control warping of the cross-sections and use has been made of the fact that $\Phi^*(\xi)$ converges faster for $\xi \leqslant 1$ than for $\xi > 1$. Also, the torsional stiffnesses B_i^* and the torques T_i are given by

$$
\begin{aligned}
&B_1^* = \frac{W^2L^2}{3}\mu^* b^*(\xi_1), \quad B_2^* = \frac{H^2L^2}{3}\mu^* b^*(\xi_2), \quad B_3^* = \frac{H^2W^2}{3}\mu^* b^*(\xi_3),\\
&T_1 = B_1^*\omega_1^*, \quad T_2 = B_2^*\omega_2^*, \quad T_3 = B_3^*\omega_3^*,\\
&\xi_1 = \mathrm{Min}\left\{\frac{W}{L}, \frac{L}{W}\right\}, \quad \xi_2 = \mathrm{Min}\left\{\frac{H}{L}, \frac{L}{H}\right\}, \quad \xi_3 = \mathrm{Min}\left\{\frac{H}{W}, \frac{W}{H}\right\},\\
&b^*(\xi) = \frac{1}{\xi}\left[1 - \frac{192}{\pi^5\xi}\sum_{n=1}^{\infty}\left[\frac{1}{(2n-1)^5}\right]\tanh\left\{\frac{\pi(2n-1)\xi}{2}\right\}\right],
\end{aligned}
\tag{7.16}
$$

where ω_i^* are the constant twists per unit length and the functions ξ_i have been specified to maximize the convergence rate of the series solutions for the stiffnesses.

In view of these results, and with the help of (5.9) and (6.4), the problem of pure torsion in the Cosserat theory is formulated by specifying

$$
\begin{aligned}
&\mathbf{m}^i = \mathbf{m}^{i*}, \quad \mathbf{b}^i = 0, \quad \boldsymbol{\delta}_0 = \boldsymbol{\delta}_1 = \boldsymbol{\delta}_2 = \boldsymbol{\delta}_3 = \boldsymbol{\delta}_7 = 0,\\
&\boldsymbol{\delta}_4 = \frac{\kappa_1^3}{L}\mathbf{e}_3, \quad \boldsymbol{\delta}_5 = \frac{\kappa_2^2}{W}\mathbf{e}_2, \quad \boldsymbol{\delta}_6 = \frac{\kappa_3^1}{H}\mathbf{e}_1,
\end{aligned}
\tag{7.17}
$$

where $\{\kappa_1^3, \kappa_2^2, \kappa_3^1\}$ are expressed in terms of the constant twists ω_i per unit length, and the warping variables Φ_i, such that

$$
\begin{aligned}
&\frac{\kappa_1^3}{L} = \omega_1 - \omega_2 - \omega_3\Phi_3, \quad \frac{\kappa_2^2}{W} = -\omega_1 + \omega_2\Phi_2 + \omega_3, \quad \frac{\kappa_3^1}{H} = -\omega_1\Phi_1 + \omega_2 - \omega_3,\\
&T_1 = B_1\omega_1, \quad T_2 = B_2\omega_2, \quad T_3 = B_3\omega_3.
\end{aligned}
\tag{7.18}
$$

Then, using (6.5), (7.5) and (7.6) the nontrivial equilibrium equations (6.3) can be solved to obtain the results

$$\begin{aligned}
B_1 &= \frac{2W^2L^2(K_{10}K_{11}K_{12} - K_{12}K_{13}K_{13} - K_{11}K_{14}K_{14} + 2K_{13}K_{14}K_{15} - K_{10}K_{15}K_{15})}{\left[\frac{W}{L}(K_{11}K_{12} - K_{15}K_{15}) + (K_{12}K_{13} - K_{14}K_{15})\right]},\\
B_2 &= \frac{2H^2L^2(K_{10}K_{11}K_{12} - K_{12}K_{13}K_{13} - K_{11}K_{14}K_{14} + 2K_{13}K_{14}K_{15} - K_{10}K_{15}K_{15})}{\left[\frac{H}{L}(K_{11}K_{12} - K_{15}K_{15}) + (K_{11}K_{14} - K_{13}K_{15})\right]},\\
B_3 &= \frac{2H^2W^2(K_{10}K_{11}K_{12} - K_{12}K_{13}K_{13} - K_{11}K_{14}K_{14} + 2K_{13}K_{14}K_{15} - K_{10}K_{15}K_{15})}{\left[\frac{H}{W}(K_{10}K_{12} - K_{14}K_{14}) + (K_{10}K_{15} - K_{13}K_{14})\right]},\\
\Phi_1 &= \frac{\left[\frac{L}{H}(K_{13}K_{14} - K_{10}K_{15}) + \frac{W}{H}(K_{11}K_{14} - K_{13}K_{15})\right]}{\left[\frac{W}{L}(K_{11}K_{12} - K_{15}K_{15}) + (K_{12}K_{13} - K_{14}K_{15})\right]},\\
\Phi_2 &= \frac{\left[\frac{H}{W}(K_{12}K_{13} - K_{14}K_{15}) + \frac{L}{W}(K_{13}K_{14} - K_{10}K_{15})\right]}{\left[\frac{H}{L}(K_{11}K_{12} - K_{15}K_{15}) + (K_{11}K_{14} - K_{13}K_{15})\right]},\\
\Phi_3 &= \frac{\left[\frac{H}{L}(K_{12}K_{13} - K_{14}K_{15}) + \frac{W}{L}(K_{13}K_{15} - K_{11}K_{14})\right]}{\left[\frac{H}{W}(K_{10}K_{12} - K_{14}K_{14}) + (K_{10}K_{15} - K_{13}K_{14})\right]},
\end{aligned} \tag{7.19}$$

together with the restrictions that

$$\begin{aligned}
&\frac{W}{L}(K_{11}K_{12} - K_{15}K_{15}) = \frac{L}{W}(K_{10}K_{12} - K_{14}K_{14}),\\
&\frac{H}{L}(K_{11}K_{12} - K_{15}K_{15}) = \frac{L}{H}(K_{10}K_{11} - K_{13}K_{13}),\\
&\frac{H}{W}(K_{10}K_{12} - K_{14}K_{14}) = \frac{W}{H}(K_{10}K_{11} - K_{13}K_{13}).
\end{aligned} \tag{7.20}$$

In contrast with the case of pure bending, it does not appear to be possible to choose values of the constitutive coefficients so that the Cosserat solution will predict exact results for pure torsion for all geometries of the rectangular parallelepiped. Consequently, some compromise has to be made. To this end, the Cosserat coefficients are specified by modifying the Bubnov–Galerkin coefficients such that

$$\begin{aligned}
&K_{10} = \frac{\mu^*}{6}\left[\frac{H^2+W^2}{L^2}\right]b^*(1), \quad K_{11} = \frac{\mu^*}{6}\left[\frac{H^2+L^2}{W^2}\right]b^*(1), \quad K_{12} = \frac{\mu^*}{6}\left[\frac{W^2+L^2}{H^2}\right]b^*(1),\\
&K_{13} = \frac{\mu^*}{6}\left[\frac{H^2}{WL}\right]b^*(1), \quad K_{14} = \frac{\mu^*}{6}\left[\frac{W^2}{HL}\right]b^*(1), \quad K_{15} = \frac{\mu^*}{6}\left[\frac{L^2}{HW}\right]b^*(1).
\end{aligned} \tag{7.21}$$

In particular, these coefficients satisfy the restrictions (7.20) and they produce the results

$$\begin{aligned}
&B_1 = \frac{\mu^* W^2 L^2}{3}\left[\frac{2b^*(1)}{\frac{W}{L}+\frac{L}{W}}\right], \quad B_2 = \frac{\mu^* H^2 L^2}{3}\left[\frac{2b^*(1)}{\frac{H}{L}+\frac{L}{H}}\right], \quad B_3 = \frac{\mu^* H^2 W^2}{3}\left[\frac{2b^*(1)}{\frac{H}{W}+\frac{W}{H}}\right],\\
&\Phi_1 = \frac{\frac{W}{L}-\frac{L}{W}}{\frac{W}{L}+\frac{L}{W}}, \quad \Phi_2 = \frac{\frac{H}{L}-\frac{L}{H}}{\frac{L}{H}+\frac{H}{L}}, \quad \Phi_3 = \frac{\frac{H}{W}-\frac{W}{H}}{\frac{H}{W}+\frac{W}{H}}.
\end{aligned} \tag{7.22}$$

The Galerkin coefficients in Table 1 also satisfy the restrictions (7.20) and when they are substituted into (7.19), they yield the same warping functions Φ_i as those in (7.22) for the Cosserat solution, but the stiffnesses B_i are different. Specifically, the functional forms of the normalized torsional stiffnesses [i.e. the associated functions in the square brackets in (7.22) for B_i, respectively] are given by

$$b^*(\xi_1), \quad C_1(\xi_1) = \frac{2b^*(1)}{\xi_1 + \frac{1}{\xi_1}}, \quad G_1(\xi_1) = \frac{1}{\xi_1 + \frac{1}{\xi_1}}, \tag{7.23}$$

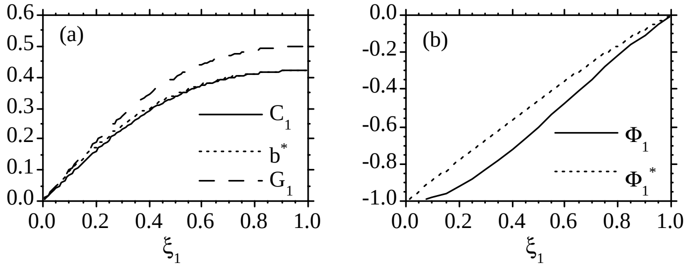

Fig. 2. (a) Normalized torsional stiffnesses predicted by the exact solution b^*, the Cosserat solution C_1 and the Bubnov–Galerkin solution G_1 and (b) warping functions predicted by the exact solution Φ_1^* and the Cosserat (and Bubnov–Galerkin) solution Φ_1.

where b^* corresponds to the exact solution (7.16), and C_1 and G_1 correspond to the Cosserat and Bubnov–Galerkin solutions, respectively. Moreover due to the symmetry of these functions the full range can be explored by considering $(0 \leqslant \xi_1 \leqslant 1)$. Fig. 2a compares these normalized torsional stiffnesses and Fig. 2b compares the warping functions Φ_1^* and Φ_1. From these figures it can be seen that the Cosserat solution for normalized torsional stiffness is quite accurate and that the Cosserat solution for warping is acceptable. Moreover, it is noted from Fig. 2a that the Bubnov–Galerkin solution has the most error for the case of a square cross-section $(\xi_1 = 1)$.

7.3. Higher-order hourglassing

The remaining constitutive coefficients $\{K_{16}\text{–}K_{18}\}$ in the strain energy function (5.10) control the stiffnesses to higher order hourglassing associated with warping. These coefficients can be determined by considering the exact equilibrium solution associated with no body force which is given by

$$\begin{aligned}
u_1^* &= 2(3-2\nu^*)C_1\theta^1\theta^2\theta^3 - C_2(\theta^1)^2\theta^3 - C_3(\theta^1)^2\theta^2,\\
u_2^* &= -C_1(\theta^2)^2\theta^3 + 2(3-2\nu^*)C_2\theta^1\theta^2\theta^3 - C_3\theta^1(\theta^2)^2,\\
u_3^* &= -C_1\theta^2(\theta^3)^2 - C_2\theta^1(\theta^3)^2 + 2(3-2\nu^*)C_3\theta^1\theta^2\theta^3,\\
T_{11}^* &= \mu^*\left[4(3-\nu^*)C_1\theta^2\theta^3 - 4(1-\nu^*)C_2\theta^1\theta^3 - 4(1-\nu^*)C_3\theta^1\theta^2\right],\\
T_{22}^* &= \mu^*\left[-4(1-\nu^*)C_1\theta^2\theta^3 + 4(3-\nu^*)C_2\theta^1\theta^3 - 4(1-\nu^*)C_3\theta^1\theta^2\right],\\
T_{33}^* &= \mu^*\left[-4(1-\nu^*)C_1\theta^2\theta^3 - 4(1-\nu^*)C_2\theta^1\theta^3 + 4(3-\nu^*)C_3\theta^1\theta^2\right],\\
T_{12}^* &= \mu^*\left[2(3-2\nu^*)C_1\theta^1\theta^3 + 2(3-2\nu^*)C_2\theta^2\theta^3 - C_3\{(\theta^1)^2+(\theta^2)^2\}\right],\\
T_{13}^* &= \mu^*\left[2(3-2\nu^*)C_1\theta^1\theta^2 - C_2\{(\theta^1)^2+(\theta^3)^2\} + 2(3-2\nu^*)C_3\theta^2\theta^3\right],\\
T_{23}^* &= \mu^*\left[-C_2\{(\theta^2)^2+(\theta^3)^2\} + 2(3-2\nu^*)C_2\theta^1\theta^2 + 2(3-2\nu^*)C_3\theta^1\theta^3\right],
\end{aligned} \tag{7.24}$$

where u_i^* are the components of the 3-D displacement vector $\mathbf{u}^*$ relative to $\mathbf{e}_i$ and $\{C_1, C_2, C_3\}$ are constants. Now, it can be shown with the help of (7.8), (7.9) and (7.10) that the values $\boldsymbol{\delta}_i^*$, $\mathbf{m}^{i*}$, and $\hat{\mathbf{m}}_J^*$ become

$$
\begin{aligned}
&\boldsymbol{\delta}_0^* = \boldsymbol{\delta}_4^* = \boldsymbol{\delta}_5^* = \boldsymbol{\delta}_6^* = 0,\\
&\boldsymbol{\delta}_1^* = \left[-\frac{W^2}{12}C_3\right]\mathbf{e}_2 + \left[-\frac{L^2}{12}C_2\right]\mathbf{e}_3, \quad \boldsymbol{\delta}_2^* = \left[-\frac{H^2}{12}C_3\right]\mathbf{e}_1 + \left[-\frac{L^2}{12}C_1\right]\mathbf{e}_3,\\
&\boldsymbol{\delta}_3^* = \left[-\frac{H^2}{12}C_2\right]\mathbf{e}_1 + \left[-\frac{W^2}{12}C_1\right]\mathbf{e}_2, \quad \boldsymbol{\delta}_7^* = 2(3-2v^*)[C_1\mathbf{e}_1 + C_2\mathbf{e}_2 + C_3\mathbf{e}_3],\\
&\mathbf{m}^{0^*} = \mathbf{m}^{4^*} = \mathbf{m}^{5^*} = \mathbf{m}^{6^*} = 0,\\
&\mathbf{m}^{1^*} = \left[-\frac{\mu^* HWL}{12}(H^2+W^2)C_3\right]\mathbf{e}_2 + \left[-\frac{\mu^* HWL}{12}(H^2+L^2)C_2\right]\mathbf{e}_3,\\
&\mathbf{m}^{2^*} = \left[-\frac{\mu^* HWL}{12}(H^2+W^2)C_3\right]\mathbf{e}_1 + \left[-\frac{\mu^* HWL}{12}(W^2+L^2)C_1\right]\mathbf{e}_3,\\
&\mathbf{m}^{3^*} = \left[-\frac{\mu^* HWL}{12}(H^2+L^2)C_2\right]\mathbf{e}_1 + \left[-\frac{\mu^* HWL}{12}(W^2+L^2)C_1\right]\mathbf{e}_2,\\
&\mathbf{m}^{7^*} = \left[\frac{\mu^* HWL}{72}\{2(3-v^*)W^2L^2 + (3-2v^*)H^2(W^2+L^2)\}C_1\right]\mathbf{e}_1\\
&\qquad + \left[\frac{\mu^* HWL}{72}\{2(3-v^*)H^2L^2 + (3-2v^*)W^2(H^2+L^2)\}C_2\right]\mathbf{e}_2\\
&\qquad + \left[\frac{\mu^* HWL}{72}\{2(3-v^*)H^2W^2 + (3-2v^*)L^2(H^2+W^2)\}C_3\right]\mathbf{e}_3.
\end{aligned} \tag{7.25}
$$

To develop the Csosserat solution it is convenient express the displacements $\boldsymbol{\delta}_i$ and $\boldsymbol{\delta}_i^*$ in terms of their components

$$
\boldsymbol{\delta}_i = \sum_{j=1}^{3} \tilde{\delta}_{ij}\mathbf{e}_j, \quad \boldsymbol{\delta}_i^* = \sum_{j=1}^{3} \tilde{\delta}_{ij}^*\mathbf{e}_j \qquad \text{for } i = 0, 1, \ldots, 7, \tag{7.26a,b}
$$

where a superposed ($\sim$) is used to avoid confusion with the components of the Kronecker delta symbol. In view of these results, the Cosserat solution is taken in the form

$$
\begin{aligned}
&\mathbf{m}^i = \mathbf{m}^{i^*}, \quad \mathbf{b}^i = 0, \quad \boldsymbol{\delta}_1 = \tilde{\delta}_{12}\mathbf{e}_2 + \tilde{\delta}_{13}\mathbf{e}_3,\\
&\tilde{\boldsymbol{\delta}}_2 = \tilde{\delta}_{21}\mathbf{e}_1 + \tilde{\delta}_{23}\mathbf{e}_3, \quad \tilde{\boldsymbol{\delta}}_3 = \tilde{\delta}_{31}\mathbf{e}_1 + \tilde{\delta}_{32}\mathbf{e}_2,\\
&\boldsymbol{\delta}_4 = \boldsymbol{\delta}_5 = \boldsymbol{\delta}_6 = 0, \quad \boldsymbol{\delta}_7 = \tilde{\delta}_{71}\mathbf{e}_1 + \tilde{\delta}_{72}\mathbf{e}_2 + \tilde{\delta}_{73}\mathbf{e}_3.
\end{aligned} \tag{7.27}
$$

Then, using (5.9), (6.4), (6.5), (7.5) and (7.6) the nontrivial equilibrium equations (6.3) can be solved and compared with the exact results (7.25) to deduce that $\{\tilde{\delta}_{71}, \tilde{\delta}_{72}, \tilde{\delta}_{73}\}$ will be exact provided that $\{K_{16}, K_{17}, K_{18}\}$ are specified by

$$
\begin{aligned}
&K_{16} = \frac{\mu^*}{144}\left[\frac{2(3-v^*)}{(3-2v^*)} + \frac{H^2}{W^2} + \frac{H^2}{L^2}\right], \quad K_{17} = \frac{\mu^*}{144}\left[\frac{2(3-v^*)}{(3-2v^*)} + \frac{W^2}{H^2} + \frac{W^2}{L^2}\right],\\
&K_{18} = \frac{\mu^*}{144}\left[\frac{2(3-v^*)}{(3-2v^*)} + \frac{L^2}{H^2} + \frac{L^2}{W^2}\right],
\end{aligned} \tag{7.28}
$$

which are different from the Bubnov–Galerkin values in Table 1. Furthermore, the other equations of equilibrium give values of the other displacement components which are related to the exact values (7.25) by the expressions

$$\frac{\tilde{\delta}_{12}}{\tilde{\delta}^*_{12}} = \frac{1}{2}\left\{1 + \frac{H^2}{W^2}\right\}, \quad \frac{\tilde{\delta}_{13}}{\tilde{\delta}^*_{13}} = \frac{1}{2}\left\{1 + \frac{H^2}{L^2}\right\},$$
$$\frac{\tilde{\delta}_{21}}{\tilde{\delta}^*_{21}} = \frac{1}{2}\left\{1 + \frac{W^2}{H^2}\right\}, \quad \frac{\tilde{\delta}_{23}}{\tilde{\delta}^*_{23}} = \frac{1}{2}\left\{1 + \frac{W^2}{L^2}\right\}, \tag{7.29}$$
$$\frac{\tilde{\delta}_{31}}{\tilde{\delta}^*_{31}} = \frac{1}{2}\left\{1 + \frac{L^2}{H^2}\right\}, \quad \frac{\tilde{\delta}_{32}}{\tilde{\delta}^*_{32}} = \frac{1}{2}\left\{1 + \frac{L^2}{W^2}\right\}.$$

Thus, it is impossible to reproduce the exact solution unless the element is a cube ($H = W = L$). Nevertheless, the hourglass coefficients will be specified by (7.28) for all dimensions of the element.

7.4. Positive definite strain energy

Using the Cosserat values of the constitutive coefficients given in Table 1 it can be shown that the strain energy function Ψ in (5.10) for inhomogeneous deformations can be rewritten in the form

$$\begin{aligned} 2m\Psi = {} & \frac{E^*HWL}{24(1-\nu^{*2})}[(1+\nu^*)\{(\kappa_1^1+\kappa_3^3)^2 + (\kappa_1^2+\kappa_2^3)^2 + (\kappa_2^1+\kappa_3^2)^2\} \\ & + (1-\nu^*)\{(\kappa_1^1-\kappa_3^3)^2 + (\kappa_1^2-\kappa_2^3)^2 + (\kappa_2^1-\kappa_3^2)^2\}] + \frac{\mu^*HWLb^*(1)}{6}\left[H^2\left\{\frac{\kappa_1^3}{L}+\frac{\kappa_2^2}{W}\right\}^2\right. \\ & \left. + W^2\left\{\frac{\kappa_1^3}{L}+\frac{\kappa_3^1}{H}\right\}^2 + L^2\left\{\frac{\kappa_2^2}{W}+\frac{\kappa_3^1}{H}\right\}^2\right] + HWL[K_{16}\{\kappa_4^1\}^2 + K_{17}\{\kappa_4^2\}^2 + K_{18}\{\kappa_4^3\}^2], \end{aligned} \tag{7.30}$$

Consequently, in view of the usual restrictions

$$\mu^* > 0, \quad -1 < \nu^* < \frac{1}{2}, \tag{7.31}$$

and the fact that $\{K_{16}, K_{17}, K_{18}\}$ are positive, it follows that Ψ is a positive definite function of its arguments.

7.5. Director inertia coefficients

Using the expression (4.4a), the Bubnov–Galerkin values of the director inertia coefficients y^{ij} are given by

$$y^{00} = 1, \quad y^{11} = \frac{H^2}{12}, \quad y^{22} = \frac{W^2}{12}, \quad y^{33} = \frac{L^2}{12}, \tag{7.32a–d}$$

$$y^{44} = \frac{H^2W^2}{(12)^2}, \quad y^{55} = \frac{H^2L^2}{(12)^2}, \quad y^{66} = \frac{W^2L^2}{(12)^2}, \quad y^{77} = \frac{H^2W^2L^2}{(12)^3}, \tag{7.32e–h}$$

$$\text{all other } y^{ij} = 0. \tag{7.32i}$$

Motivated these values, it is assumed in the Cosserat theory that (7.32a) and (7.32i) hold, but the remaining coefficients

$$\{y^{11}, y^{22}, y^{33}, y^{44}, y^{55}, y^{66}, y^{77}\}, \tag{7.33}$$

need to be determined by matching solutions of vibration problems. Specifically, attention is focused on free-vibrations of the element. Apart from notational changes, it can be shown that the equations for extensional vibrations and shear vibrations are the same as those already analyzed in (Rubin, 1986). The work their indicates that $\{y^{11}, y^{22}, y^{33}\}$ should be specified by

$$y^{11} = \frac{H^2}{\pi^2}, \quad y^{22} = \frac{W^2}{\pi^2}, \quad y^{33} = \frac{L^2}{\pi^2}, \tag{7.34}$$

instead of the Bubnov–Galerkin values (7.32b,c,d). In principle, the remaining values of y^{ij} could be determined by comparing with the exact solution of Hutchinson and Zillmer (1983), but this is not pursued here due to the complexity of that solution. Until this more complete analysis is done, it is tempting use the relationships between the Cosserat values (7.34) and the Bubnov–Galerkin values (7.32b,c,d) to modify the Bubnov–Galerkin values (7.32f,g,h) and specify

$$y^{44} = \frac{H^2 W^2}{\pi^4}, \quad y^{55} = \frac{H^2 L^2}{\pi^4}, \quad y^{66} = \frac{W^2 L^2}{\pi^4}, \quad y^{77} = \frac{H^2 W^2 L^2}{\pi^6}. \tag{7.35}$$

8. Nodal forms of the balance laws

In the Cosserat theory developed in the previous sections it has been most convenient to express the equations of motions and the constitutive equations in terms of the director quantities $\mathbf{d}_i$ $(i = 0, 1, \ldots, 7)$. This was particularly useful in expressing the restrictions (5.5) associated with 3-D homogeneous deformations. In contrast, in the finite element method the equations are usually expressed in terms of nodal variables. Specifically, using the definitions (3.5) the director velocities $\mathbf{w}_i$ can be expressed in terms of the nodal velocities $\bar{\mathbf{w}}_i = \dot{\bar{\mathbf{d}}}_i$. Furthermore, by introducing the definitions

$$\bar{y}^{ij} = \bar{y}^{ji} = \sum_{r=0}^{7} \sum_{s=0}^{7} A_{ri} y^{rs} A_{sj}, \quad \bar{\mathbf{b}}^i = \sum_{r=0}^{7} A_{ri} \mathbf{b}^r, \tag{8.1a,b}$$

$$\bar{\mathbf{m}}^i_J = \sum_{r=0}^{7} A_{ri} \mathbf{m}^r_J \ (J = 1, 2, \ldots 6), \quad \bar{\mathbf{m}}^i = \sum_{r=0}^{7} A_{ri} \mathbf{m}^r, \quad \bar{\mathbf{t}}^i = \sum_{r=0}^{7} A_{ri} \mathbf{t}^r, \tag{8.1c–e}$$

the director momentum equations (2.4b) can be written in the nodal forms

$$\frac{\mathrm{d}}{\mathrm{d}t}\left[\sum_{j=0}^{7} m \bar{y}_{ij} \bar{\mathbf{w}}_j\right] = m\bar{\mathbf{b}}^i + \bar{\mathbf{m}}^i - \bar{\mathbf{t}}^i \quad (i = 0, 1, \ldots, 7), \tag{8.2}$$

where $\bar{\mathbf{b}}^i$ are specific nodal body forces, $\bar{\mathbf{m}}^i$ are nodal contact forces, and $\bar{\mathbf{t}}^i$ are nodal internal forces [unlike $\mathbf{t}^0$ in (2.4b), the nodal vector $\bar{\mathbf{t}}^0$ does not necessarily vanish]. Also, it can be shown that energy quantities (2.6) can be written in their nodal forms

$$\begin{gathered}\mathscr{K} = \sum_{i=0}^{7} \sum_{j=0}^{7} \frac{1}{2} m \bar{y}^{ij} \bar{\mathbf{w}}_i \cdot \bar{\mathbf{w}}_j, \quad \mathscr{W} = \mathscr{W}_{\mathrm{b}} + \mathscr{W}_{\mathrm{c}}, \\ \mathscr{W}_{\mathrm{b}} = \sum_{i=0}^{7} m \bar{\mathbf{b}}^i \cdot \bar{\mathbf{w}}_i, \quad \mathscr{W}_{\mathrm{c}} = \sum_{i=0}^{7} \bar{\mathbf{m}}^i \cdot \bar{\mathbf{w}}_i,\end{gathered} \tag{8.3}$$

where $\mathscr{W}_{\mathrm{b}}$ is the rate of work of nodal body forces and $\mathscr{W}_{\mathrm{c}}$ is the rate of work of nodal contact forces. In particular, it is important to emphasize that although the nodal equations are written in terms of nodal quantities, the constitutive equations for $\bar{\mathbf{t}}^i$ are most conveniently expressed as functions $\mathbf{t}^i$ which depend directly on director variables.

Moreover, using the definitions (4.4c,d) and the results (4.7), it follows that the eight vectors $\bar{\mathbf{m}}^i$ are defined in terms of the 24 independent vectors in the set $\mathbf{m}^i_J$. Specifically, the external nodal forces $\bar{\mathbf{m}}^i$ can be expressed in the forms

$$
\begin{aligned}
\bar{\mathbf{m}}^0 &= \int_{\partial P_4}\left[\frac{1}{4}-\frac{\theta^2}{2W}-\frac{\theta^3}{2L}+\frac{\theta^2\theta^3}{WL}\right]\mathbf{t}^*\mathrm{d}a^* + \int_{\partial P_5}\left[\frac{1}{4}-\frac{\theta^1}{2H}-\frac{\theta^3}{2L}+\frac{\theta^1\theta^3}{HL}\right]\mathbf{t}^*\mathrm{d}a^* \\
&\quad + \int_{\partial P_6}\left[\frac{1}{4}-\frac{\theta^1}{2H}-\frac{\theta^2}{2W}+\frac{\theta^1\theta^2}{HW}\right]\mathbf{t}^*\mathrm{d}a^*, \\
\bar{\mathbf{m}}^1 &= \int_{\partial P_1}\left[\frac{1}{4}-\frac{\theta^2}{2W}-\frac{\theta^3}{2L}+\frac{\theta^2\theta^3}{WL}\right]\mathbf{t}^*\mathrm{d}a^* + \int_{\partial P_5}\left[\frac{1}{4}+\frac{\theta^1}{2H}-\frac{\theta^3}{2L}-\frac{\theta^1\theta^3}{HL}\right]\mathbf{t}^*\mathrm{d}a^* \\
&\quad + \int_{\partial P_6}\left[\frac{1}{4}+\frac{\theta^1}{2H}-\frac{\theta^2}{2W}-\frac{\theta^1\theta^2}{HW}\right]\mathbf{t}^*\mathrm{d}a^*, \\
\bar{\mathbf{m}}^2 &= \int_{\partial P_1}\left[\frac{1}{4}+\frac{\theta^2}{2W}-\frac{\theta^3}{2L}-\frac{\theta^2\theta^3}{WL}\right]\mathbf{t}^*\mathrm{d}a^* + \int_{\partial P_2}\left[\frac{1}{4}+\frac{\theta^1}{2H}-\frac{\theta^3}{2L}-\frac{\theta^1\theta^3}{HL}\right]\mathbf{t}^*\mathrm{d}a^* \\
&\quad + \int_{\partial P_6}\left[\frac{1}{4}+\frac{\theta^1}{2H}+\frac{\theta^2}{2W}+\frac{\theta^1\theta^2}{HW}\right]\mathbf{t}^*\mathrm{d}a^*, \\
\bar{\mathbf{m}}^3 &= \int_{\partial P_2}\left[\frac{1}{4}-\frac{\theta^1}{2H}-\frac{\theta^3}{2L}+\frac{\theta^1\theta^3}{HL}\right]\mathbf{t}^*\mathrm{d}a^* + \int_{\partial P_4}\left[\frac{1}{4}+\frac{\theta^2}{2W}-\frac{\theta^3}{2L}-\frac{\theta^2\theta^3}{WL}\right]\mathbf{t}^*\mathrm{d}a^* \\
&\quad + \int_{\partial P_6}\left[\frac{1}{4}-\frac{\theta^1}{2H}+\frac{\theta^2}{2W}-\frac{\theta^1\theta^2}{HW}\right]\mathbf{t}^*\mathrm{d}a^*, \\
\bar{\mathbf{m}}^4 &= \int_{\partial P_3}\left[\frac{1}{4}-\frac{\theta^1}{2H}-\frac{\theta^2}{2W}+\frac{\theta^1\theta^2}{HW}\right]\mathbf{t}^*\mathrm{d}a^* + \int_{\partial P_4}\left[\frac{1}{4}-\frac{\theta^2}{2W}+\frac{\theta^3}{2L}-\frac{\theta^2\theta^3}{WL}\right]\mathbf{t}^*\mathrm{d}a^* \\
&\quad + \int_{\partial P_5}\left[\frac{1}{4}-\frac{\theta^1}{2H}+\frac{\theta^3}{2L}-\frac{\theta^1\theta^3}{HL}\right]\mathbf{t}^*\mathrm{d}a^*, \\
\bar{\mathbf{m}}^5 &= \int_{\partial P_1}\left[\frac{1}{4}-\frac{\theta^2}{2W}+\frac{\theta^3}{2L}-\frac{\theta^2\theta^3}{WL}\right]\mathbf{t}^*\mathrm{d}a^* + \int_{\partial P_3}\left[\frac{1}{4}+\frac{\theta^1}{2H}-\frac{\theta^2}{2W}-\frac{\theta^1\theta^2}{HW}\right]\mathbf{t}^*\mathrm{d}a^* \\
&\quad + \int_{\partial P_5}\left[\frac{1}{4}+\frac{\theta^1}{2H}+\frac{\theta^3}{2L}+\frac{\theta^1\theta^3}{HL}\right]\mathbf{t}^*\mathrm{d}a^*, \\
\bar{\mathbf{m}}^6 &= \int_{\partial P_1}\left[\frac{1}{4}+\frac{\theta^2}{2W}+\frac{\theta^3}{2L}+\frac{\theta^2\theta^3}{WL}\right]\mathbf{t}^*\mathrm{d}a^* + \int_{\partial P_2}\left[\frac{1}{4}+\frac{\theta^1}{2H}+\frac{\theta^3}{2L}+\frac{\theta^1\theta^3}{HL}\right]\mathbf{t}^*\mathrm{d}a^* \\
&\quad + \int_{\partial P_3}\left[\frac{1}{4}+\frac{\theta^1}{2H}+\frac{\theta^2}{2W}+\frac{\theta^1\theta^2}{HW}\right]\mathbf{t}^*\mathrm{d}a^*, \\
\bar{\mathbf{m}}^7 &= \int_{\partial P_2}\left[\frac{1}{4}-\frac{\theta^1}{2H}+\frac{\theta^3}{2L}-\frac{\theta^1\theta^3}{HL}\right]\mathbf{t}^*\mathrm{d}a^* + \int_{\partial P_3}\left[\frac{1}{4}-\frac{\theta^1}{2H}+\frac{\theta^2}{2W}-\frac{\theta^1\theta^2}{HW}\right]\mathbf{t}^*\mathrm{d}a^* \\
&\quad + \int_{\partial P_4}\left[\frac{1}{4}+\frac{\theta^2}{2W}+\frac{\theta^3}{2L}+\frac{\theta^2\theta^3}{WL}\right]\mathbf{t}^*\mathrm{d}a^*.
\end{aligned}
\tag{8.4}
$$

Thus, with the help of Fig. 1 it can be seen that each external nodal force is influenced only by surface tractions on the three surfaces ∂P_J which intersect that node.

Furthermore, for the linear theory it is assumed that the nodal vectors $\bar{\mathbf{d}}_i$ can be expressed in the forms

$$\bar{\mathbf{d}}_i = \overline{\mathbf{D}}_i + \bar{\boldsymbol{\delta}}_i \quad (i = 0, 1, \ldots, 7), \tag{8.5}$$

where $\overline{\mathbf{D}}_i$ are the reference values of $\bar{\mathbf{d}}_i$, and $\bar{\boldsymbol{\delta}}_i$ are displacements. In addition, it is assumed that these displacements and the kinetic quantities

$$\{\bar{\mathbf{b}}^i, \bar{\mathbf{m}}^i, \bar{\mathbf{t}}^i\} \quad (i = 0, 1, \ldots, 7) \tag{8.6}$$

remain small enough that quadratic terms in these quantities can be neglected relative to linear terms. It then follows that the linearized forms of equations of motion (8.2) can be written as

$$\sum_{j=0}^{7} m\bar{y}^{ij}\ddot{\bar{\boldsymbol{\delta}}}_j = m\bar{\mathbf{b}}^i + \bar{\mathbf{m}}^i - \bar{\mathbf{t}}^i \quad (i = 0, 1, \ldots, 7). \tag{8.7}$$

9. Numerical solution procedure

The theory of a Cosserat point developed in the previous sections can be used to formulate the numerical solution of 3-D problems in nonlinear elasticity. Just as in the standard finite element procedure, the body is modeled as a collection of M elements which interact through their common boundaries. Here, the Ith element ($I = 1, 2, \ldots, M$) is modeled as a Cosserat point with boundaries ${}_I\partial P_J$ ($J = 1, 2, \ldots, 6$).

In general, the Cosserat theory allows the element in its stress-free reference configuration to be a general eight node brick element. The values of the constitutive coefficients $\{K_1–K_{18}\}$ developed in Section 7 were determined for the special case when the reference shape is a rectangular parallelepiped. Nevertheless, the tensorial structure of the theory is used to generalize the equations for general brick elements. Although, additional research is required to determine the accuracy of this generalization, the resulting theory is valid for nonlinear deformations of a general brick element.

The kinematics and kinetics of the Ith Cosserat point are characterized by the nodal equations of Section 8 with a subscript I added to the left of each quantity (including the lengths H, W, L) and with no implied sum on repeated upper cased indices. Specifically, the directors ${}_I\mathbf{d}_i$, the director velocities ${}_I\mathbf{w}_i$, the nodal directors ${}_I\bar{\mathbf{d}}_i$ and nodal director velocities ${}_I\bar{\mathbf{w}}_i$ of the Ith element are denoted by

$${}_I\mathbf{d}_i, \quad {}_I\mathbf{w}_i = {}_I\dot{\mathbf{d}}_i, \quad {}_I\bar{\mathbf{d}}_i, \quad {}_I\bar{\mathbf{w}}_i = {}_I\dot{\bar{\mathbf{d}}}_i \qquad (I = 1, 2, \ldots, M) \ (i = 0, 1, \ldots, 7). \tag{9.1}$$

Also, the nodal equations of director momentum (8.2) of the Ith element become

$$\sum_{j=0}^{7} {}_Im_I\bar{y}^{ij}\,{}_I\dot{\bar{\mathbf{w}}}_j = {}_Im_I\bar{\mathbf{b}}^i + {}_I\bar{\mathbf{m}}^i - {}_I\bar{\mathbf{t}}^i \qquad (I = 1, 2, \ldots, M) \ (i = 0, 1, \ldots, 7), \tag{9.2}$$

where the constitutive equations for the nodal internal forces ${}_I\bar{\mathbf{t}}^i$ are determined by the formulas developed in the previous sections and the nodal contact forces ${}_I\bar{\mathbf{m}}^i$ are determined by formulas of the type (8.4).

For a given topology of the body, the M elements are characterized by N global nodes which are located relative to a fixed origin by the global position vectors $\mathbf{d}^*_K$ ($K = 1, 2, \ldots, N$). Consequently, the Cosserat points are connected by the kinematic coupling conditions

$$\left\{{}_I\bar{\mathbf{d}}_0 \text{ or } {}_I\bar{\mathbf{d}}_1 \text{ or } {}_I\bar{\mathbf{d}}_2 \text{ or } {}_I\bar{\mathbf{d}}_3 \text{ or } {}_I\bar{\mathbf{d}}_4 \text{ or } {}_I\bar{\mathbf{d}}_5 \text{ or } {}_I\bar{\mathbf{d}}_6 \text{ or } {}_I\bar{\mathbf{d}}_7\right\} = \mathbf{d}^*_K \quad (K = 1, 2, \ldots, N). \tag{9.3}$$

The Cosserat points are also connected by the kinetic coupling conditions

$$\sum_{(I,i:K)} {}_I\bar{\mathbf{m}}^i = \mathbf{m}^*_K, \tag{9.4}$$

where $\mathbf{m}_K^*$ are nodal external concentrated forces, and the special summation symbol indicates that the summation is performed over all forces i $(i = 0, 1, \ldots, 7)$ and all elements I $(I = 1, 2, \ldots, M)$ which have nodes that coincide with the Kth node. Next, solving the equations of motion (9.2) for ${}_I\bar{\mathbf{m}}^i$, these kinetic coupling conditions can be rewritten in the forms

$$\sum_{(I,i:K)} \left[\sum_{j=0}^{7} {}_I m_I \bar{y}^{ij} {}_I\dot{\bar{\mathbf{w}}}_j - {}_I m_I \bar{\mathbf{b}}^i + {}_I\bar{\mathbf{t}}^i \right] = \mathbf{m}_K^* \quad (K = 1, 2, \ldots, N). \tag{9.5}$$

If the Kth node is an interior node then expressions of the type (8.4) indicate that the external nodal forces due to the elements that have the common node K are associated with the common boundaries that intersect that node. Consequently, since the traction vector is a linear function of the outward normal, it follows that the external nodal force $\mathbf{m}_K^*$ vanishes for interior nodes

$$\mathbf{m}_K^* = 0 \quad \text{for interior nodes } K. \tag{9.6}$$

At an exterior node K the value of $\mathbf{m}_K^*$ is specified by

$$\mathbf{m}_K^* = \sum_{(I,i:K)} [{}_I\bar{\mathbf{m}}^i]_{\text{Ext}}, \tag{9.7}$$

where the value of $[{}_I\bar{\mathbf{m}}^i]_{\text{Ext}}$ is determined by expressions of the type (8.4) with the only nonzero terms being those associated with the exterior surfaces that intersect the node K.

The discretized equations of motion (9.5) represent N vector ordinary differential equations to determine the N nodal vectors $\mathbf{d}_K^*$ as functions of time. Since these equations are second-order in time it follows that initial conditions must be specified of the forms

$$\mathbf{d}_K^*(0) = \text{specified}, \quad \dot{\mathbf{d}}_K^*(0) = \text{specified}. \tag{9.8}$$

The boundary conditions associated with the global body under consideration appear in the equations of motion (9.5) tacitly through the nodal contact forces $\mathbf{m}_K^*$. To analyze the nature of these conditions it is convenient to use (8.3) to express the rate of work done on the Ith element due to nodal contact forces in the form

$${}_I\mathscr{W}_{\text{c}} = \sum_{i=0}^{7} {}_I\bar{\mathbf{m}}^i \cdot {}_I\bar{\mathbf{w}}_i. \tag{9.9}$$

Consequently, with the help of the coupling equations (9.3) and (9.4), the rate of work done on the entire body due to contact forces can be written as

$$\mathscr{W}_{\text{c}} = \sum_{I=1}^{M} {}_I\mathscr{W}_{\text{c}} = \sum_{K=1}^{N} \mathbf{m}_K^* \cdot \dot{\mathbf{d}}_K^*. \tag{9.10}$$

It therefore follows that the work due to surface tractions is done on the body only through external nodal forces applied to external nodes. Specifically, the boundary conditions can be specified at each external node as kinematic conditions

$$\mathbf{d}_K^*(t) = \text{specified}, \tag{9.11}$$

with $\mathbf{m}_K^*$ being determined by the equations of motions, or kinetic conditions

$$\mathbf{m}_K^*(t) = \text{specified}, \tag{9.12}$$

with $\mathbf{d}_K^*$ being determined by the equations of motion, or by mixed–mixed boundary conditions where some components of $\mathbf{d}_K^*$ and the other components of $\mathbf{m}_K^*$ are specified at the same node K.

10. Large deformation uniaxial stress

It is well known (Wriggers and Reese, 1996; Reese and Wriggers, 2000; Reese et al., 2000; Wall et al., 2000) that standard finite elements for nonlinear elasticity can lose stiffness to hourglassing when they are severely compressed. Here, it is shown that the Cosserat point developed in the previous sections does not exhibit this unphysical phenomena. To this end, consider the large deformation associated with uniaxial uniform Cauchy stress T_{33}^* acting in the $\mathbf{e}_3$ direction on the block shown in Fig. 3. In order to explore the effects of potential hourglassing, a nonlinear deformation is considered for which the nodal vectors are given by

$$\begin{aligned}
&\mathbf{d}_1^* = -\frac{bH}{2}\mathbf{e}_1 - \frac{bW}{2}\mathbf{e}_2 - \delta\mathbf{e}_2, \quad \mathbf{d}_2^* = -\frac{bW}{2}\mathbf{e}_2 - \delta\mathbf{e}_2, \\
&\mathbf{d}_3^* = \frac{bH}{2}\mathbf{e}_1 - \frac{bW}{2}\mathbf{e}_2 - \delta\mathbf{e}_2, \quad \mathbf{d}_4^* = \frac{bH}{2}\mathbf{e}_1 + \delta\mathbf{e}_2, \\
&\mathbf{d}_5^* = \frac{bH}{2}\mathbf{e}_1 + \frac{bW}{2}\mathbf{e}_2 - \delta\mathbf{e}_2, \quad \mathbf{d}_6^* = \frac{bW}{2}\mathbf{e}_2 - \delta\mathbf{e}_2, \\
&\mathbf{d}_7^* = -\frac{bH}{2}\mathbf{e}_1 + \frac{bW}{2}\mathbf{e}_2 - \delta\mathbf{e}_2, \quad \mathbf{d}_8^* = -\frac{bH}{2}\mathbf{e}_1 + \delta\mathbf{e}_2, \quad \mathbf{d}_9^* = \delta\mathbf{e}_2, \\
&\mathbf{d}_K^* = \mathbf{d}_{K-9}^* + \frac{aL}{2}\mathbf{e}_3 + 2\delta\mathbf{e}_2 \quad (K = 10, 11, 12, 14, 15, 16), \\
&\mathbf{d}_K^* = \mathbf{d}_{K-9}^* + \frac{aL}{2}\mathbf{e}_3 - 2\delta\mathbf{e}_2 \quad (K = 13, 17, 18), \\
&\mathbf{d}_K^* = \mathbf{d}_{K-18}^* + aL\mathbf{e}_3 \quad (K = 19, 20, \ldots, 27),
\end{aligned} \tag{10.1}$$

where δ characterizes the magnitude of hourglassing (Fig. 4) and a and b are stretches associated with the underlying homogeneous deformation ($\delta = 0$). Now, using the fact that the dimensions of the Ith element are specified by

$${}_IH = \frac{H}{2}, \quad {}_IW = \frac{W}{2}, \quad {}_IL = \frac{L}{2}, \tag{10.2}$$

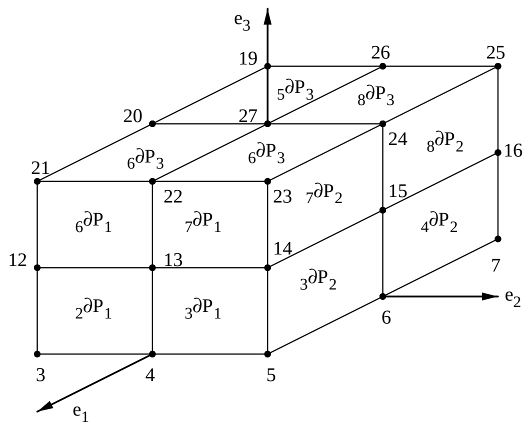

Fig. 3. Sketch of a 3-D block discretized by eight elements showing the global numbering of the nodes and the element numbering of the exposed surfaces.

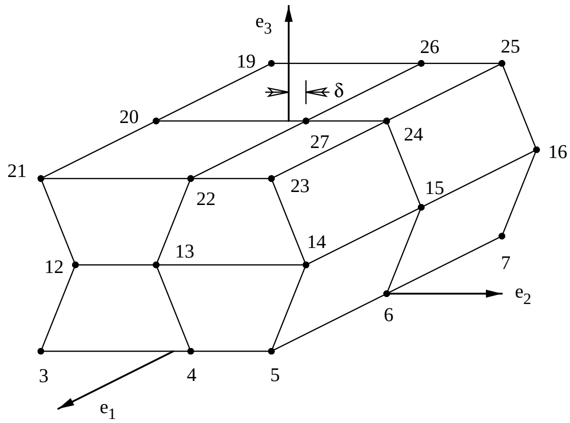

Fig. 4. Sketch of nonlinear deformation of a 3-D block with assumed hourglass modes.

it can be shown that the directors ${}_I\mathbf{d}_i$ in the Ith element are given by

$$
\begin{aligned}
&{}_1\mathbf{d}_0 = \frac{1}{4}[-bH\mathbf{e}_1 - bW\mathbf{e}_2 + aL\mathbf{e}_3], \quad {}_2\mathbf{d}_0 = \frac{1}{4}[bH\mathbf{e}_1 - bW\mathbf{e}_2 + aL\mathbf{e}_3],\\
&{}_3\mathbf{d}_0 = \frac{1}{4}[bH\mathbf{e}_1 + bW\mathbf{e}_2 + aL\mathbf{e}_3], \quad {}_4\mathbf{d}_0 = \frac{1}{4}[-bH\mathbf{e}_1 + bW\mathbf{e}_2 + aL\mathbf{e}_3],\\
&{}_I\mathbf{d}_0 = {}_{I-4}\mathbf{d}_0 + \frac{1}{2}aL\mathbf{e}_3 \quad \text{for } I = 5,6,7,8,\\
&{}_I\mathbf{d}_1 = b\mathbf{e}_1, \quad {}_I\mathbf{d}_2 = b\mathbf{e}_2, \quad {}_I\mathbf{d}_3 = a\mathbf{e}_3, \quad {}_I\mathbf{d}_4 = {}_I\mathbf{d}_5 = {}_I\mathbf{d}_7 = 0 \quad \text{for } I = 1,2,\ldots,8,\\
&{}_I\mathbf{d}_6 = -\frac{16}{WL}\delta\mathbf{e}_2 \quad \text{for } I = 1,2,7,8, \quad {}_I\mathbf{d}_6 = \frac{16}{WL}\delta\mathbf{e}_2 \quad \text{for } I = 3,4,5,6.
\end{aligned}
\tag{10.3}
$$

Moreover, the reference values ${}_I\mathbf{D}_i$ of the directors are given by

$$
{}_I\mathbf{D}_1 = \mathbf{e}_1, \quad {}_I\mathbf{D}_2 = \mathbf{e}_2, \quad {}_I\mathbf{D}_3 = \mathbf{e}_3, \quad {}_I\mathbf{D}_4 = {}_I\mathbf{D}_5 = {}_I\mathbf{D}_6 = {}_I\mathbf{D}_7 = 0 \qquad \text{for } I = 1,2,\ldots,8, \tag{10.4}
$$

so that with the help of (10.2) and the kinematical definitions (2.8), (2.9) and (5.9), it can be shown that

$$
\begin{aligned}
&{}_I\mathbf{F} = b(\mathbf{e}_1 \otimes \mathbf{e}_1 + \mathbf{e}_2 \otimes \mathbf{e}_2) + a(\mathbf{e}_3 \otimes \mathbf{e}_3), \quad J = ab^2, \quad {}_I\boldsymbol{\beta}_1 = {}_I\boldsymbol{\beta}_2 = {}_I\boldsymbol{\beta}_4 = 0 \quad \text{for } I = 1,2,\ldots,8,\\
&{}_I\boldsymbol{\beta}_3 = -\frac{16}{bWL}\delta\mathbf{e}_2 \quad \text{for } I = 1,2,7,8, \quad {}_I\boldsymbol{\beta}_3 = \frac{16}{bWL}\delta\mathbf{e}_2 \quad \text{for } I = 3,4,5,6,\\
&{}_I\kappa_1^i = {}_I\kappa_2^i = {}_I\kappa_4^i = 0 \quad \text{for } I = 1,2,\ldots,8 \quad \text{and} \quad i = 1,2,3,\\
&{}_I\kappa_3^1 = {}_I\kappa_3^3 = 0 \quad \text{for } I = 1,2,\ldots,8,\\
&{}_I\kappa_3^2 = -\frac{8}{bW}\delta \ \text{ for } I = 1,2,7,8, \quad {}_I\kappa_3^2 = \frac{8}{bW}\delta \ \text{ for } I = 3,4,5,6.
\end{aligned}
\tag{10.5}
$$

Furthermore, using (2.13c), (5.7), (5.11), (7.6), (10.2) and using the Cosserat material constants in Table 1 (with H, W, L replaced by ${}_IH$, ${}_IW$, ${}_IL$), the constitutive equations for each element can be written in the forms

$$
\begin{aligned}
{}_I d^{1/2}{}_I\mathbf{T} &= \frac{HWL}{8}\left[K^*(J-1)\mathbf{I} + \frac{\mu^*(b^2-a^2)}{3J^{2/3}}\{(\mathbf{e}_1\otimes\mathbf{e}_1+\mathbf{e}_2\otimes\mathbf{e}_2)-2(\mathbf{e}_3\otimes\mathbf{e}_3)\}\right],\\
{}_I\mathbf{t}^0 &= {}_I\mathbf{t}^4 = {}_I\mathbf{t}^7 = 0, \quad {}_I\mathbf{t}^1 = \frac{HWL}{8b}\left[K^*(J-1)+\frac{\mu^*(b^2-a^2)}{3J^{2/3}}\right]\mathbf{e}_1,\\
{}_I\mathbf{t}^2 &= \frac{HWL}{8b}\left[K^*(J-1)+\frac{\mu^*(b^2-a^2)}{3J^{2/3}}\right]\mathbf{e}_2 - \left[\frac{2v^*E^*HL}{3(1-v^{*2})b^3}\right]\delta^2\mathbf{e}_2,\\
{}_I\mathbf{t}^3 &= \frac{HWL}{8a}\left[K^*(J-1)-\frac{2\mu^*(b^2-a^2)}{3J^{2/3}}\right]\mathbf{e}_3 \quad \text{for } I=1,2,\ldots,8,\\
{}_I\mathbf{t}^5 &= -\left\{\frac{v^*E^*HWL^2}{24(1-v^{*2})b^2}\right\}\delta\mathbf{e}_1, \quad {}_I\mathbf{t}^6 = -\left\{\frac{v^*E^*HWL^2}{24(1-v^{*2})b^2}\right\}\delta\mathbf{e}_2 \quad \text{for } I=1,2,7,8,\\
{}_I\mathbf{t}^5 &= \left\{\frac{v^*E^*HWL^2}{24(1-v^{*2})b^2}\right\}\delta\mathbf{e}_1, \quad {}_I\mathbf{t}^6 = \left\{\frac{v^*E^*HWL^2}{24(1-v^{*2})b^2}\right\}\delta\mathbf{e}_2 \quad \text{for } I=3,4,5,6.
\end{aligned}
\tag{10.6}
$$

For the problem under consideration, body force is neglected, and the top ($\theta^3 = L$) and bottom ($\theta^3 = 0$) surfaces are considered to be frictionless parallel planes with the vertical ($\mathbf{e}_3$) distance between them being controlled by the stretch a. Also, the lateral surfaces ($\theta^1 = \pm H/2$; $\theta^2 = \pm W/2$) are traction free with the magnitude of the stretch b being determined by the solution of the problem. Consequently, the external nodal forces $\mathbf{m}_K^*$ satisfy the conditions

$$
\begin{aligned}
&\mathbf{m}_K^*\cdot\mathbf{e}_1 = 0, \quad \mathbf{m}_K^*\cdot\mathbf{e}_2 = 0 \qquad \text{for } K = 1\text{–}9, 19\text{–}27\\
&\mathbf{m}_K^* = 0 \quad \text{for } K = 10\text{–}18,
\end{aligned}
\tag{10.7}
$$

where the vertical components of the external nodal forces on the top and bottom surfaces are determined by the solution of the problem.

Next, the solution must satisfy each of the kinetic coupling equation (9.5). However, in order to show that the solution of this problem necessarily corresponds to homogeneous deformation with no hourglass mode ($\delta = 0$) it is sufficient to consider the equation of equilibrium at the exterior node $K = 10$. Specifically, it can be shown that the kinetic equation (9.5) corresponding to ($K = 10$) reduces to

$$
\begin{aligned}
&-\frac{1}{W}\left[\frac{HWL}{8b}\left\{K^*(J-1)+\frac{\mu^*(b^2-a^2)}{3J^{2/3}}\right\}\mathbf{e}_2 - \left\{\frac{2v^*E^*HL}{3(1-v^{*2})b^3}\right\}\delta^2\mathbf{e}_2\right] + \frac{4}{HL}\left\{\frac{v^*E^*HWL^2}{24(1-v^{*2})b^2}\right\}\delta\mathbf{e}_1\\
&\quad + \frac{4}{WL}\left\{\frac{v^*E^*HWL^2}{24(1-v^{*2})b^2}\right\}\delta\mathbf{e}_2 = 0,
\end{aligned}
\tag{10.8}
$$

which can be solved to deduce that

$$
\delta = 0, \quad K^*(J-1) + \frac{\mu^*(b^2-a^2)}{3J^{2/3}} = 0. \tag{10.9a, b}
$$

The first equation indicates that the hourglass mode necessarily vanishes for all values of the stretch a, and the second equation is used to determine the value of b for a specified value of a. Consequently, the resulting solution is consistent with the exact solution for homogeneous deformation of the block.

11. Summary

The theory of a Cosserat point has been used to formulate a new 3-D finite element for the numerical analysis of dynamic problems in nonlinear elasticity. Within the context of the direct approach to the development of the Cosserat theory, the Cosserat point is characterized by eight director vectors which are determined by balance laws and constitutive equations. For hyperelastic response, the constitutive equations for the director couples are determined by derivatives of a strain energy function. Restrictions are imposed on the strain energy function which ensure that the element satisfies a nonlinear version of the patch test.

The kinematics of this element are consistent with the standard tri-linear approximation in an eight-node brick element. Nodal equations have been developed which are assembled using common finite element methods based on kinematic and kinetic coupling at common nodes. Specifically, the nodal equations represent a system of ordinary differential equations which depend on time only. These equations can be integrated using standard numerical methods to determine the dynamic response of a nonlinear elastic body.

It has been shown that the Cosserat balance laws are in one-to-one correspondence with those obtained using a Bubnov–Galerkin formulation. Nevertheless, there is an essential difference between the two approaches in the procedure for obtaining the strain energy function. Specifically, the constitutive coefficients for inhomogeneous deformations in the Cosserat approach are determined by comparison with exact solutions or experimental data. In contrast, the Bubnov–Galerkin approach determines these constitutive coefficients by integrating the 3-D strain energy function using the kinematic approximation.

The constitutive coefficients in Table 1 cause the Cosserat theory to predict exact results for pure bending and accurate results for pure torsion of a rectangular parallelepiped, even in the limit that the element becomes a thin plate. In contrast, the constitutive coefficients associated with the Bubnov–Galerkin approach yield an incorrect response even for a cube and they exhibit unphysical stiffness for pure bending in this plate limit. Also, it is known (e.g. Simo et al., 1993) that the Bubnov–Galerkin coefficients exhibit locking for bending in the incompressible limit when $v^* = 1/2$ [i.e. the Bubnov–Galerkin coefficients $\{K_1–K_9\}$ in Table 1 become infinite]. In contrast, the Cosserat coefficients $\{K_1–K_9\}$ in Table 1 remain finite so this locking is absent in the Cosserat theory.

Although the constitutive coefficients for inhomogeneous deformations in the Cosserat theory were determined by comparison with exact linear solutions, the resulting theory is valid for large deformations. Furthermore, the tensorial structure of the Cosserat theory is used model general reference geometry of the brick element. With the help of this nonlinear theory it has also been shown that the Cosserat theory eliminates unphysical hourglassing in large compression without the need for using assumed enhanced strains or special weighting functions. This result is partially due to the specific nonlinear kinematic variables that are introduced in the Cosserat theory.

Ultimately, the response of the finite element formulation is dependent on the functional form of the strain energy and not on the specific procedure used to obtain it. Consequently, the Cosserat approach, which proposes a functional form of the strain energy directly in terms of the independent variables, yields an efficient use of the reduced number of degrees of freedom in the element. Also, it appears that the same 3-D element can be used in the limit of thin plates.

Acknowledgements

The research of M.B. Rubin was partially supported by the fund for the promotion of research at the Technion. Also, the authors would like to thank Prof. C. Sansour for calling our attention to the hourglassing instability in large compression.

Appendix A. Transformation matrix for the nodal representation

Using the numbering system shown in Fig. 1, the transformation matrix A_{ij} in (3.5) is given by

$$\begin{aligned}
A_{0j} &= \frac{1}{8}\{1,1,1,1,1,1,1,1\},\\
A_{1j} &= \frac{1}{4H}\{-1,1,1,-1,-1,1,1,-1\},\\
A_{2j} &= \frac{1}{4W}\{-1,-1,1,1,-1,-1,1,1\},\\
A_{3j} &= \frac{1}{4L}\{-1,-1,-1,-1,1,1,1,1\},\\
A_{4j} &= \frac{1}{2HW}\{1,-1,1,-1,1,-1,1,-1\},\\
A_{5j} &= \frac{1}{2HL}\{1,-1,-1,1,-1,1,1,-1\},\\
A_{6j} &= \frac{1}{2WL}\{1,1,-1,-1,-1,-1,1,1\},\\
A_{7j} &= \frac{1}{HWL}\{-1,1,-1,1,1,-1,1,-1\}.
\end{aligned} \tag{A.1}$$

Appendix B. Details of homogeneous deformations

The quantities V and $\mathbf{V}^i$ in (5.1) and the restrictions (5.2) associated with the nonlinear patch test for homogeneous deformations are related to integrals over the region P_0 occupied by the point in its reference configuration by the formulas

$$D^{1/2}V = \int_{P_0} \mathrm{d}V^*, \quad D^{1/2}V\mathbf{V}^i = \sum_{m=1}^{3} \int_{P_0} [N^{(i+3)}_{,m}\mathbf{G}^m]\,\mathrm{d}V^* \quad (i = 1,2,3,4), \tag{B.1}$$

where $\mathrm{d}V^* = G^{1/2}\,\mathrm{d}\theta^1\,\mathrm{d}\theta^2\,\mathrm{d}\theta^3$ is the reference element of volume and the reciprocal vectors $\mathbf{G}^i$ are defined in (4.3). Specifically, using the kinematic representation (3.1) and defining P_0 by (3.4), these integrals yield the expressions

$$\begin{aligned}
D^{1/2}V &= HWL\left[D^{1/2} + \frac{H^2}{12}\mathbf{D}_4\times\mathbf{D}_5\cdot\mathbf{D}_1 + \frac{W^2}{12}\mathbf{D}_6\times\mathbf{D}_4\cdot\mathbf{D}_2 + \frac{L^2}{12}\mathbf{D}_5\times\mathbf{D}_6\cdot\mathbf{D}_3\right],\\
D^{1/2}V\mathbf{V}^1 &= HWL\left[\frac{H^2}{12}\mathbf{D}_5\times\mathbf{D}_1 + \frac{W^2}{12}\mathbf{D}_2\times\mathbf{D}_6\right],\\
D^{1/2}V\mathbf{V}^2 &= HWL\left[\frac{H^2}{12}\mathbf{D}_1\times\mathbf{D}_4 + \frac{L^2}{12}\mathbf{D}_6\times\mathbf{D}_3\right],\\
D^{1/2}V\mathbf{V}^3 &= HWL\left[\frac{W^2}{12}\mathbf{D}_4\times\mathbf{D}_2 + \frac{L^2}{12}\mathbf{D}_3\times\mathbf{D}_5\right], \quad D^{1/2}V\mathbf{V}^4 = 0.
\end{aligned} \tag{B.2}$$

Appendix C. Determination of the Bubnov–Galerkin coefficients

Using the kinematic approximation (7.7) it follows that the linearized 3-D strain tensor $\mathbf{E}^*$ can be expressed in the form

$$
\begin{aligned}
\mathbf{E}^* &= \sum_{i=1}^{3} \frac{1}{2}\left[\frac{\partial \mathbf{u}^*}{\partial \theta^i} \otimes \mathbf{e}_i + \mathbf{e}_i \otimes \frac{\partial \mathbf{u}^*}{\partial \theta^i}\right] = \sum_{i=0}^{6} N^i \mathbf{E}_i, \\
\mathbf{E}_0 &= \mathbf{E} = \frac{1}{2}[\boldsymbol{\delta}_1 \otimes \mathbf{e}_1 + \mathbf{e}_1 \otimes \boldsymbol{\delta}_1 + \boldsymbol{\delta}_2 \otimes \mathbf{e}_2 + \mathbf{e}_2 \otimes \boldsymbol{\delta}_2 + \boldsymbol{\delta}_3 \otimes \mathbf{e}_3 + \mathbf{e}_3 \otimes \boldsymbol{\delta}_3], \\
\mathbf{E}_1 &= \frac{1}{2}[\boldsymbol{\delta}_4 \otimes \mathbf{e}_2 + \mathbf{e}_2 \otimes \boldsymbol{\delta}_4 + \boldsymbol{\delta}_5 \otimes \mathbf{e}_3 + \mathbf{e}_3 \otimes \boldsymbol{\delta}_5], \\
\mathbf{E}_2 &= \frac{1}{2}[\boldsymbol{\delta}_4 \otimes \mathbf{e}_1 + \mathbf{e}_1 \otimes \boldsymbol{\delta}_4 + \boldsymbol{\delta}_6 \otimes \mathbf{e}_3 + \mathbf{e}_3 \otimes \boldsymbol{\delta}_6], \\
\mathbf{E}_3 &= \frac{1}{2}[\boldsymbol{\delta}_5 \otimes \mathbf{e}_1 + \mathbf{e}_1 \otimes \boldsymbol{\delta}_5 + \boldsymbol{\delta}_6 \otimes \mathbf{e}_2 + \mathbf{e}_2 \otimes \boldsymbol{\delta}_6], \\
\mathbf{E}_4 &= \frac{1}{2}[\boldsymbol{\delta}_7 \otimes \mathbf{e}_3 + \mathbf{e}_3 \otimes \boldsymbol{\delta}_7], \quad \mathbf{E}_5 = \frac{1}{2}[\boldsymbol{\delta}_7 \otimes \mathbf{e}_2 + \mathbf{e}_2 \otimes \boldsymbol{\delta}_7], \quad \mathbf{E}_6 = \frac{1}{2}[\boldsymbol{\delta}_7 \otimes \mathbf{e}_1 + \mathbf{e}_1 \otimes \boldsymbol{\delta}_7].
\end{aligned}
\tag{C.1}
$$

Next, for the linear theory of an elastically isotropic material, the 3-D strain energy function corresponding to (5.6) becomes

$$
\rho_0^* \Sigma^*(\mathbf{E}^*) = \frac{1}{2} K^* (\mathbf{E}^* \cdot \mathbf{I})^2 + \mu^* \mathbf{E}^{*\prime} \cdot \mathbf{E}^{*\prime} = \mu^* \left[\left\{\frac{v^*}{1 - 2v^*}\right\}(\mathbf{E}^* \cdot \mathbf{I})^2 + \mathbf{E}^* \cdot \mathbf{E}^*\right], \quad \mathbf{E}^{*\prime} = \mathbf{E}^* - \frac{1}{3}(\mathbf{E}^* \cdot \mathbf{I})\mathbf{I}.
\tag{C.2}
$$

Consequently, for the rectangular parallelepiped discussed in Section 8 the strain energy (4.6) can be rewritten in the form

$$
m\Sigma = \int_{-L/2}^{L/2} \int_{-W/2}^{W/2} \int_{-H/2}^{H/2} \rho_0^* \Sigma^*(\mathbf{E}^*)\, \mathrm{d}\theta^1\, \mathrm{d}\theta^2\, \mathrm{d}\theta^3,
\tag{C.3}
$$

which yields

$$
\begin{aligned}
m\Sigma &= m\Sigma^*(\mathbf{E}) + m\Psi, \\
m\Psi &= \frac{H^2}{12} m\Sigma^*(\mathbf{E}_1) + \frac{W^2}{12} m\Sigma^*(\mathbf{E}_2) + \frac{L^2}{12} m\Sigma^*(\mathbf{E}_3) \\
&\quad + \frac{H^2 W^2}{144} m\Sigma^*(\mathbf{E}_4) + \frac{H^2 L^2}{144} m\Sigma^*(\mathbf{E}_5) + \frac{W^2 L^2}{144} m\Sigma^*(\mathbf{E}_6).
\end{aligned}
\tag{C.4}
$$

Also, with the help of (5.9), (6.4) and (7.6) it can be shown that

$$
\begin{aligned}
\boldsymbol{\delta}_4 &= \frac{\kappa_1^1}{W}\mathbf{e}_1 + \frac{\kappa_1^2}{H}\mathbf{e}_2 + \frac{\kappa_1^3}{L}\mathbf{e}_3, \quad \boldsymbol{\delta}_5 = \frac{\kappa_2^1}{L}\mathbf{e}_1 + \frac{\kappa_2^2}{W}\mathbf{e}_2 + \frac{\kappa_2^3}{H}\mathbf{e}_3, \\
\boldsymbol{\delta}_6 &= \frac{\kappa_3^1}{H}\mathbf{e}_1 + \frac{\kappa_3^2}{L}\mathbf{e}_2 + \frac{\kappa_3^3}{W}\mathbf{e}_3, \quad \boldsymbol{\delta}_7 = \frac{\kappa_4^1}{WL}\mathbf{e}_1 + \frac{\kappa_4^2}{HL}\mathbf{e}_2 + \frac{\kappa_4^3}{HW}\mathbf{e}_3.
\end{aligned}
\tag{C.5}
$$

Next, comparison of (C.4) with the expression (7.15) yields the Bubnov–Galerkin coefficients given in Table 1.

References

Cohen, H., 1981. Pseudo-rigid bodies. Utilitas Math. 20, 221–247.

Cohen, H., Muncaster, R.G., 1984a. The dynamics of pseudo-rigid bodies: general structure and exact solutions. J. Elastic. 14, 127–154.

Cohen, H., Muncaster, R.G., 1984b. Theory of Pseudo-rigid Bodies. Springer, Berlin.

Flory, P., 1961. Thermodynamic relations for high elastic materials. Trans. Faraday Soc. 57, 829–838.
Green, A.E., Adkins, J.E., 1960. Large Elastic Deformations and Non-linear Continuum Mechanics. Oxford University Press, London.
Huebner, K.H., 1975. The Finite Element Method for Engineers. John Wiley, New York.
Hutchinson, J.R., Zillmer, S.D., 1983. Vibration of a free rectangular parallelepiped. ASME J. Appl. Mech. 50, 123–130.
Lekhnitskii, S.G., 1963. Theory of Elasticity of an Anisotropic Elastic Body. Holden-Day, San Francisco.
Muncaster, R.G., 1984. Invariant manifolds in mechanics I: zero-dimensional elastic bodies with directors. Arch. Ration. Mech. Analysis 84, 353–373.
Naghdi, P.M., Rubin, M.B., 1995. Restrictions on nonlinear constitutive equations for elastic shells. J. Elastic. 39, 133–163.
Papadopoulos, P., 2001. On a class of higher-order pseudo-rigid bodies. Math. Mech. Solids 6, 631–640.
Reese, S., Wriggers, P., 2000. A stabilization technique to avoid hourglassing in finite elasticity. Int. J. Numer. Meth. Engng. 48, 79–109.
Reese, S., Wriggers, P., Reddy, B.D., 2000. A new locking-free brick element technique for large deformation problems in elasticity. Compt. Struct. 75, 291–304.
Rubin, M.B., 1985a. On the theory of a Cosserat point and its application to the numerical solution of continuum problems. ASME J. Appl. Mech. 52, 368–372.
Rubin, M.B., 1985b. On the numerical solution of one-dimensional continuum problems using the theory of a Cosserat point. ASME J. Appl. Mech. 52, 373–378.
Rubin, M.B., 1986. Free vibration of a rectangular parallelepiped using the theory of a Cosserat point. ASME J. Appl. Mech. 53, 45–50.
Rubin, M.B., 1987a. On the numerical solution of nonlinear string problems using theory of a Cosserat point. Int. J. Solids Struct. 23, 335–349.
Rubin, M.B., 1987b. On the numerical solution of spherically symmetric problems using the theory of a Cosserat surface. Int. J. Solids Struct. 23, 335–349.
Rubin, M.B., 1995. Numerical solution of two- and three-dimensional thermomechanical problems using the theory of a Cosserat point. J. Math. Phys ZAMP 46, Special Issue S308–S334. In: Casey J., Crochet, M.J. (Eds.), Theoretical, Experimental, and Numerical Contributions to the Mechanics of Fluids and Solids, Birkhouser Verlag, Basel.
Rubin, M.B., 1996. Restrictions on nonlinear constitutive equations for elastic rods. J. Elastic. 44, 9–36.
Rubin, M.B., 2000. In: Cosserat Theories: Shells, Rods and Points Solid Mechanics and its Applications, vol. 79. Kluwer, The Netherlands.
Rubin, M.B., 2001. Numerical solution procedures for nonlinear elastic rods using the theory of a Cosserat point. Int. J. Solids Struct. 38, 4395–4437.
Rubin, M.B., 2002. On the quest for the best Timoshenko shear coefficient. ASME J. Appl. Mech. 70, 154–157.
Rubin, M.B., Gottlieb, O., 1996. Numerical solutions of forced vibration and whirling of a non-linear string using the theory of a Cosserat point. J. Sound Vibrat. 197, 85–101.
Slawianowski, J.J., 1974. Analytical mechanics of finite homogeneous strains. Arch. Mech. 26, 569–587.
Slawianowski, J.J., 1975. Newtonian dynamics of homogeneous strains. Arch. Mech. 26, 569–587.
Slawianowski, J.J., 1982. The mechanics of the homogeneously deformable body. Dynamical models with high symmetries. S. Angew. Math. Mech. 62, 229–240.
Simo, J.C., Armero, F., Taylor, R.L., 1993. Improved versions of assumed enhanced strain tri-linear elements for 3D finite deformation problems. Comput. Methods Appl. Mech. Engng. 110, 359–386.
Sokolnikoff, I.S., 1956. Mathematical Theory of Elasticity. McGraw-Hill, New York.
Solberg, J.M., Papadopoulos, P., 1999. A simple finite element-based framework for the analysis of elastic pseudo-rigid bodies. Int. J. Numer. Meth. Engng. 45, 1297–1314.
Wall, W.A., Bischoff, M., Ramm, E., 2000. A deformation dependent stabilization technique, exemplified by EAS elements at large strains. Comput. Methods Appl. Mech. Engng. 188, 859–871.
Wozniak, CZ., 1971. Basic concepts of the theory of discrete elasticity. Bull. Acad. Pol. Sci. 19, 753–758.
Wozniak, CZ., 1973a. Equations of motion and laws of conservation in the discrete elasticity. Arch. Mech. 25, 155–163.
Wozniak, CZ., 1973b. Discrete elastic Cosserat media. Arch. Mech. 25, 119–136.
Wriggers, P., Reese, S., 1996. A note on enhanced strain methods for large deformations. Comput. Methods Appl. Mech. Engng. 135, 201–209.